UNIVERSITÀ DEGLI STUDI DI PADOVA

DIPARTIMENTO DI INGEGNERIA INDUSTRIALE

CORSO DI LAUREA MAGISTRALE IN INGEGNERIA CHIMICA E DEI PROCESSI INDUSTRIALI

Tesi di Laurea Magistrale in

Ingegneria Chimica e dei Processi Industriali

DESIGN OF AN EFFICIENT CO_2 SUPPLY SYSTEM FOR MICROALGAE GROWTH IN MICROPHOTOBIOREACTORS

Relatore: Prof. Fabrizio Bezzo
Correlatrice: Dott.ssa Eleonora Sforza

Laureanda: ALESSANDRA PIAZZA

ANNO ACCADEMICO 2017 – 2018

Riassunto

La necessità di trovare alternative economicamente valide ai carburanti di fonte fossile, ha avviato negli ultimi decenni un'intensa ricerca nell'ambito della produzione di biocarburanti derivanti da biomasse microalgali. Le microalghe presentano infatti, un'alta velocità di crescita rispetto alle piante superiori terrestri e sono in grado di contenere al loro interno grandi quantità di oli. La produzione di biomassa per via fotosintetica, ha dei notevoli vantaggi dal punto di vista ambientale. Contribuisce infatti alla diminuzione dell'immissione in atmosfera dei gas serra e all'eliminazione di sali di fosforo e di ammonio dalle acque di scarico. Inoltre possono essere utilizzate per l'assorbimento di CO_2 atmosferica e per ottenere oltre ai biocarburanti, integratori alimentari, prodotti di interesse chimico e farmaceutico, mangimi per acquacoltura. Le microalghe, in aggiunta, possono essere coltivate in zone dedicate e marginali evitando così di sottrarre risorse alle coltivazioni terrestri per fini alimentari. Nonostante l'alto potenziale teorico, la produzione di biomassa algale su larga scala risulta attualmente non competitiva in termini economici. A tal fine lo studio riguardante i diversi parametri di crescita, nelle diverse condizioni ambientali, risulta essere un tema di particolare attualità.

L'introduzione in campo scientifico di dispositivi microfluidici, rappresenta un'ottima alternativa ai classici metodi di ricerca, in quanto permettono di velocizzare la raccolta dei dati dando la possibilità di effettuare molti esperimenti in parallelo, riducendo così, tempi e costi. Questo si traduce, in questo campo specifico, nella possibilità di valutare l'influenza di diversi parametri sia fisici che chimici sulla crescita microalgale mantenendo un'alta affidabilità sperimentale e al tempo stesso un alto rendimento (*high-throughput*).

Nella tesi viene descritta la progettazione di un efficiente sistema di fornitura di CO_2 per la crescita microalgale in dispositivi microfluidici (microfotobioreattori).

La prima parte del lavoro è dedicata allo studio dell'anidride carbonica come fattore limitante per lo sviluppo della biomassa, in seguito a questo, si è reso necessario uno studio sull'equilibrio carbonico dell'acqua, maggior costituente del medium di coltura. La necessità di valutare la capacità di assorbimento di CO_2 da parte del medium di coltura in funzione della concentrazione di sali è stata espletata mediante una serie di simulazioni svolte con il simulatore di processo Aspen Plus®. Un nuovo microfotobioreattore è stato progettato al fine di ottenere risultati sperimentali apprezzabili. Sono state sperimentate inoltre diverse condizioni di crescita mediante l'utilizzo di diversi terreni di cultura, valutando infine l'interazione di questo fattore con l'intensità luminosa.

I risultati ottenuti dalle prove sperimentali condotte sulla specie *Scenedesmus obliquus* hanno evidenziato che un medium di coltura arricchito con carbonato di sodio permette un assorbimento maggiore di anidride carbonica con conseguente aumento della crescita

microalgale. In ultimo, la crescita della biomassa è stata misurata a diverse intensità di luce per verificare la risposta delle alghe nel microfotobioreattore in diverse condizioni operative.

Abstract

Microalgae processes emerged during the last decade as one of the most promising new technologies for providing innovative molecules for the cosmetics and pharmaceutical industry. At a large time horizon, microalgae will contribute for fossil carbon replacement with renewable carbon, especially for supply green chemistry and liquid biofuels in the transport sector.

The optimization of the microalgae productivity still requires intense investigation, as well as numerous and time-consuming experiments. In this scenario, microscale technologies are emerging as a valuable tool to improve data production and, accordingly, to speed up the optimization process maintaining a high experimental reliability.

The goal of the Thesis is the design of an efficient CO_2 supply system for microalgae growth in microphotobioreactors (micro-PBR).

In first place, the CO_2 as a limiting factor for the microalgae growth has been studied in a microfluidic device. Once addressed this topic, the capacity of CO_2 absorption by the culture medium has been assessed by means of a series of simulations carried out with the Aspen Plus® process simulator. Secondly, new micro-PBR has been used to evaluate the influence of different culture medium on the microalgae growth. A tentative to quantify the microalgae growth is accomplished thanks to chlorophyll fluorescence intensity. Finally, a new experiment has been carried out to evaluate, in an early stage, the effect on the growth of different light intensities.

Contents

Introduction

Microalgae processes emerged during the last decade as one of the most promising new technologies for providing innovative molecules for cosmetic and pharmaceutical industry and as a source of proteins for animal and human nutrition (Mata *et al.*, 2010). At a large time horizon, microalgae will contribute for fossil carbon replacement with renewable carbon, especially for supply green chemistry and liquid biofuel in the transport sector (Foley *et al.* 2011). The great interest in this technology is not only related to the substantial higher productivity compared to the terrestrial plants (Chisti, 2007), but also to the possibility of coupling the microalgal production process to industrial CO_2 mitigation and wastewater treatments to finally recycle carbon, phosphorous and nitrogen. Nevertheless, much research is still needed in order to make this potential new energy source a real feasible technology, since all the existing techno-economic assessments are limited by uncertainties regarding the biomass productivity that can actually be reached at full-scale. The optimization of their productivity by assessing the impact that several environmental factors have on microalgae growth still requires intense investigation, as well as numerous and time-consuming experiments. In this scenario, microscale technologies are emerging as a valuable tool to improve data production and accordingly to speed up the optimization process, while maintaining a high experimental reliability.

The aim of this Thesis is the design of an efficient CO_2 supply system for microalgae in a microphotobioreactors (micro-PBR).

The work is developed in four Chapters, described below.

Chapter 1 offers a general overview of the microalgae, giving an overall classification, the conditions of growth and the main cultivation technologies. Then follows a brief summary of industrial applications, finally, at the end of the chapter the Thesis objective will be illustrated.

Chapter 2 introduces the concepts of microfluidic technology and microfluidic device, then are listed the materials and equipment that allowed the preparation of the experiments. This Chapter ends with the description of the monitoring methods used to quantify the microalgae growth, e.g. *in vivo* chlorophyll fluorescence measurements and the protocols used in the experimental phase.

Chapter 3 describes the study on carbon dioxide as a limiting factor for microalgal growth, after which a survey on the carbon balance of water is considered. Through the use of the process simulator Aspen Plus®, the absorption capacity of CO_2 by the culture medium is evaluated, which is considered mostly composed by water. The data obtained from the simulations have been elaborated in appropriate plots, with the aim to obtain an experimental protocol for the CO_2 absorption. The final part of the Chapter shows the experimental

validation of the protocol carried out at the laboratory and the development of the final prototype of the micro-PBR.

Chapter 4 summarizes the experiments carried out and the data obtained, in this sense different growth conditions have been tested, with different culture medium and different light intensities in order to obtain the optimal growth condition.

The work is concluded by drawing some final remarks and by suggesting potential direction for the future research.

Chapter 1

Context and motivation

In this chapter, the reader will be introduced to the world of microalgae, giving a short glimpse of the numerous fields of application. The phenomenon of photosynthesis will be explained in detail, which will allows a clearer understanding of the whole elaborate. Last but not least the objectives of this work will be addressed, giving a general introduction to the main steps that have characterized this research activity.

1.1 Introduction

Microalgae (also called phytoplankton) are microscopic (1-50 μm), unicellular/multicellular, prokaryotic/eukaryotic photosynthetic organism that can produce biomass and oxygen by using sunlight as energy source, inorganic salts as nutrients and carbon dioxide as carbon source. Microalgae are present in all terrestrial ecosystems, both aquatic and terrestrial, representing a large variety of species able to live in very different systems. It is estimated that there are between 200 000 and 800 000 species, but only a few of these have been studied extensively. These organisms have the ability to grow in extreme environmental conditions, scarcity of nutrients and water. The growth rate and the maximum biomass production of microalgae cultures do not depend uniquely on light, since the microalgae culture is also affected by abiotic (salinity, oxygen, pH, salinity, nutrients, temperature and toxic chemicals), biotic (pathogens and competition by other algae), and operational (mixing, depth control) factors (Mata *et al*., 2010). Depending on the species, microalgae are able to produce varying amounts of lipids, polyunsaturated fatty acid, natural dye, carotenoid, antioxidant, enzyme polymer, peptide, toxin and sterols (Medipally *et al.*, 2015). For these reasons, microalgae have generated a lot of interest due to their undoubted potential for the production of biomass and lipids through photosynthesis. In the last two decades, the search for new bio-energy feedstocks create a boom in scientific research on microalgae cultivation, which has improved the state of art of the technology at a rapid pace. However, large scale production still faces significant bottlenecks, which increase manufacturing costs and prevent microalgae from becoming a feasible bioenergy source (Sano Coelho, 2017). Therefore, despite the instability of the petrol market and the need to tackle problems such as global warming, large-scale production remains scarcely economical at the moment. For this reason, many researches are oriented towards an

optimization of mass production, in order to obtain a new technology, less impacting at an environmental level and economically sustainable.

1.1.1 Classification

As previously mentioned, there are thousands of microalgal species, from a more general point of view algae are divided into two main groups. The first group is represented by macroalgae and comprehend the red and brown algae belong, the second group comprehend the microalgae to which the diatoms, the green, golden, yellow-green and blue algae belong.

- **Red algae** (*Rhodophyta*, Figure 1.1a): are red because of the presence of the pigment phycoerythrin, this pigment reflects red light and absorb blue light. Blue light penetrates water to a greater depth than light of longer wavelengths, these pigments allow red algae to photosynthesize and live at somewhat greater depths than most other algae. Some rhodophytes have very little phycoerythrin and may appear green or bluish from the chlorophyll and other pigments present in them. In Asia this type of algae are important sources of food, such a nori. The high vitamin protein content of this food makes it attractive, as does the relative simplicity of cultivation, which began in Japan more than 300 years ago. In some Pacific atolls, red algae have contributed far more to reef structure than other organism, even more than corals These reef-building rhodophytes are called coralline algae, because they are secreted a hard shell of carbonate around themselves, in much the same way that corals do (UCMP, 2018a).

- **Brown algae** (*Phaeophyta*, Figure 1.1b): the brown colour of these algae results from the dominance of the xanthophyll pigment fucoxanthin, which masks the other pigments, chlorophyll a and c, β-carotene and other xanthophylls and count approximately 200 species. They are the most complex forms algae, commonly adapted in the marine environment. The length of brown algae can range from a microscopic length to several meters. The longest size measured is bout 30 meters. Food reserves are typically complex polysaccharides, sugar and higher alcohols. The principal carbohydrate reserve is laminarin and mannitol, and true starch is absent compare with the green algae. The walls are made of cellulose and alginic acid, a long-chained heteropolysaccharide. There are no known unicellular or colonial representatives; the simplest plant form is a branched, filamentous thallus. Most brown algae have an alternation of haploid a diploid generation. The brown Giant Kelp *Macrocystis pyrifeta* is harvested off the coasts of California for feeding abalone and it was used for alginate extraction (UCMP, 2018b).

- **Diatom** (*Bacillariophyceae*, Figure 1.2a): count approximately about 16 000 specie found in sediments or attached to solid substances in all the waters of Earth. Diatoms are among the most important and prolific microscopic sea organisms and serve directly or indirectly as food for many animals. They may be either unicellular or colonial. The silicified cell wall forms a pillbox-like shell (frustule) composed of overlapping halves (epitheca and hypotheca) perforated by intricate and delicate patterns. Food is stored as oil droplets, and the golden-brown pigment fucoxanthin masks the chlorophyll an carotenoid divided into two orders on the basis of symmetry and shape: the round nonmotile *Centrales* have radial markings and the elongated *Pennales*, which move with a gliding motion, have pinnate markings (*Encyclopaedia* Britannica, 2018a).

- **Green algae** (*Chlophyta*, Figure 1.2b): is the most diverse group of algae, with more then 7 000 species growing in a variety of habitats. The green algae is a paraphyletic group because it excludes the plantae. Like the plants, the green algae contain two forms of chlorophyll, which they use to capture light energy to fuel the manufacture of sugar, but unlike plants they are primarily aquatic (*Encyclopaedia* Britannica, 2018b).

- **Golden algae** (*Chrysophyta*, figure 1.2c): are common microscopic chromists in fresh water. Some species are colourless, but the vast majority are photosynthetic. As such, they are particularly important in lakes, where they may be the primary source of food for zooplankton. They are not considered truly autotrophic by some biologists because nearly all chrysophytes become facultatively heterotrophic in the absence of adequate light, or in the presence of plentiful dissolved food. When this occurs, the *Chrysophytes* atrophies and the algae ma turn predator, feeding on bacteria or diatoms. There are more than a thousand described species of golden algae, most of them free-swimming and unicellular, but there are filamentous and colonial forms. The colonies grow as branched or unbranched chains (*Encyclopaedia* Britannica, 2018c).

- **Yellow-green algae** (*Xanthophyta*, Figure 1.2d): include more than 600 species. Members of this group are photosynthetic organisms which live primary in fresh water, though some are found in marine waters, in damp soil, or on tree trunks. They generally are not abundant when they are found at all, and many species have only been found once. Despite this, they are the dominant producers in some salt marshes, and some, like *Tribonema*, are cosmopolitan in their distribution. Unlike the other Chromista, the yellow-green algae completely lack the brown pigment fucoxanthin. Like these other chromists however they lack chlorophyll b and instead have chlorophyll c. This gives them a characteristic yellow-green colour, as opposed to the golden colour or their relatives, which my make them difficult to recognize as chromist. They are

distinguished by their food reserve (oil), the quantity of β-carotene in their plastids, and motile cells with unequal flagella (*Encyclopaedia* Britannica, 2018d).

- **Blue-green algae** (Figure 1.2e): are types of bacteria know as **Cyanobacteria**, which occur naturally in habitats such as rivers, lakes, damp soil, tree trunks. They are aquatic and photosynthetic, live in the water and can manufactures their own food. Because they are quite small and usually unicellular, though they often grow in colonies large enough to see. They are also important providers of nitrogen fertilizer in the cultivation of rice and beans. The Cyanobacteria have also been tremendously important in shaping the course of evolution and ecological change throughout earth's history. The oxygen atmosphere that we depend on was generated by numerous cyanobacteria during the Archaean and Proterozoic Eras. The other great contribution is the origin of plants. The chloroplast with which plants make food for themselves is actually a *cyanobacterium* living within the plant's cells. During the Proterozoic, or in the early Cambrian, Cyanobacteria began to take up residence with certain eukaryote cells, making food for the eukaryote host in return for a home. This event is known as endosymbiosis and is also the origin of the eukaryotic mitochondrion. Cyanobacteria produce a number of nuisance compounds, including those that are toxic or cause severe taste and odours problems in drinking water supplies. Blue-green algae are a common and natural component of the microscope plants (plankton) in lakes and they are one of the largest and most important groups of bacteria on earth. Cyanobacteria are very important organisms for the health and growth of many plants. They are one of very few groups of organisms that can convert inert atmospheric nitrogen into an organic form, such as nitrate or ammonia. *Spirulina* is blue-green algae, has long been valued as a food source; it is high in protein, and can be cultivated in pounds quite easily. In tropical countries, it may be a very important part of the diet and was eaten regularly by the Aztecs; it also served in several Oriental dishes (UCMP, 2018c).

(a) (b)

Figure 1.1 (a) *red algae (https://www.livestrong.com/article/),* (b) *brown algae (https://www.123rf.com/stock-photo/brown_algae).*

(a)

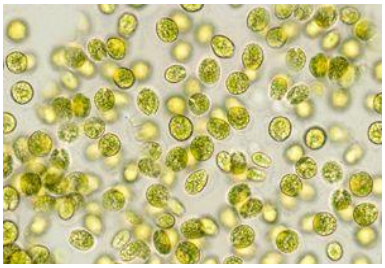

(b)

(c)

(d)

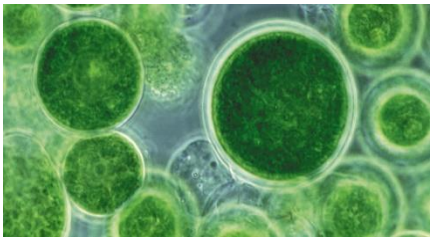

(e)

Figure 1.2 (a) *Diatom (https://nualgiaquarium.com/nano-silica-diatoms/),*
(b) *Green algae (http://www.nilesbio.com),*
(c) *Golden algae (https://www.flickr.com/photos/micromundus),*
(d) *Yellow-green algae (https://www.flickr.com/photos/micromundus),*
(e) *Blue-green algae (https://gizmodo.com).*

1.1.2 Nutritional modes and nutrient requirements

The possible nutritional routes for algae are show in Figure 1.3 Autotrophic organism obtain their energy through the absorption of light energy for the reduction of CO_2 by the oxidation of substrates, mainly water, with the release of O_2. Photoautotrophic organisms only require inorganic mineral ions and obligate photoautotrophs are those that cannot grow in the dark. By far, most algae belong to this category, although many require minimal quantities of organic compounds for growth, such as vitamins. Phototrophic cultivation is currently one of the most investigated and adopted for the large-scale microalgae biomass production; it means that the key fundamental process responsible of microalgae-based chemical energy generation is photosynthesis.

Heterotrophic organisms obtain their material and energy needs from organic compounds produced by other organisms. Several algal species can be grown exclusively on organic

substrates and this has become a viable option in conventional closed bioreactor production systems for biomass and biocompounds. Photoheterotrophic organisms require light as energy source to use organic compounds as nutrient and these organic compounds may also satisfy the energy requirements of the algae. Auxotrophy is where the algae require only small quantities of essential organic compounds such vitamins and amino acids. Mixotrophic growth is equivalent to autotrophy and heterotrophy, where both organic compounds and CO_2 are necessary for growth. A definite switch between autotrophy and heterotrophy is not manifested and both processes are present, except in total darkness (Richmond, 2004).

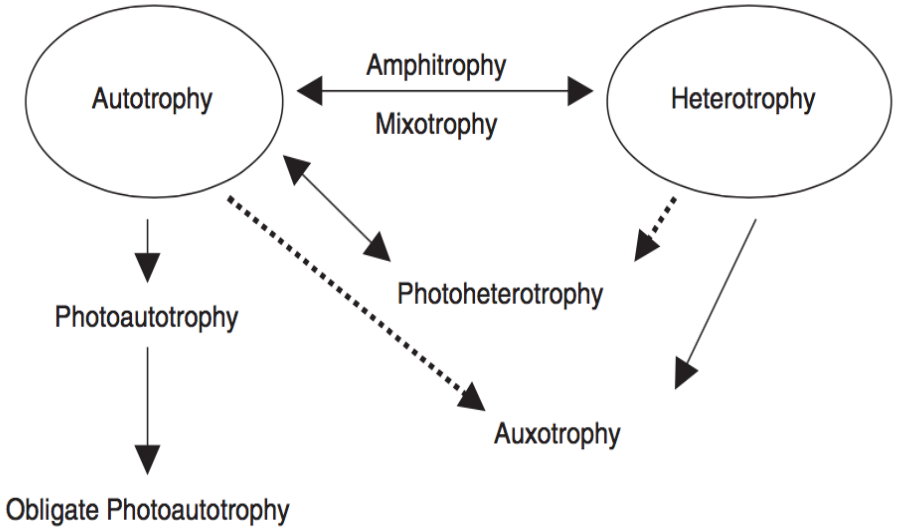

Figure 1.3 *Various trophic possibilities for algae, where autotrophic and heterotrophic growth are the most important ones. (Richmond, 2004)*

As previously mentioned many factors influence microalgae growth, these are divided into abiotic (light, temperature, concentration of nutrients, oxygen, carbon dioxide, pH, salinity and presence of toxic substance), biotic as competition with other species and presence of pathogens (bacteria, fungi) and operational factors of growth such as mixing.

As regards the required nutrients, for high rates of autotrophic production, supply of CO_2 and HCO_3^- is most important. Contrary to land plants, atmospheric cannot satisfy the carbon requirements of high yielding autotrophic algal production system. The CO_2-H_2CO_3-HCO_3^--CO_3^{2-} system is the most important buffer generally present in freshwaters and it is the best means available to control and maintain specific pH levels that are optimal for mass-cultivated species. The bicarbonate-carbonate buffer system can provide CO_2 for photosynthesis through the following reactions (Stephen, 1999):

$$2HCO_3^- \leftrightarrow CO_3^{2-} + H_2O + CO_2 \qquad (1.1)$$

$$HCO_3^- \leftrightarrow CO_2 + OH^- \quad (1.2)$$

$$CO_3^{2-} + H_2O \leftrightarrow CO_2 + 2OH^- \quad (1.3)$$

These reactions imply that during photosynthetic CO_2 fixation, OH^- accumulates in the growth solutions leading to a graduate rise in pH. After carbon, nitrogen is the most important nutrient contributing to the biomass produced. The nitrogen content of biomass can range from 1% to more than 10%. A typical response due to a nitrogen limitation is discoloration of the cells (the chlorophyll decreases while the carotenoids increase) and accumulation of organic carbon compounds such as polysaccharides and oils (Becker, 1994). Nitrogen is mostly supplied in the culture medium as nitrate, but also as ammonia or urea. Ammonia nitrogen is often the preferred N-source for microalgae and the assimilation of either NO_3^- or NH_4^+ is related to the pH of the growth media. Using ammonia as the only source of nitrogen, the pH could drop significantly during the growth phase, due to a release of H^+ ions. Phosphorus is essential for growth and many cellular processes such as energy transfer, biosynthesis of nucleic acids and DNA. The preferred form in which it is supplied to algae is as orthophosphate (PO_4^{2-}) and its uptake is energy dependent. Although algal biomass contains less than 1% phosphorus, in microalgae cultures it is often one of the major limiting factors of growth. This happens because it easily binds to other ions and precipitates with them, because of the precipitation the algae can no longer absorb it. Besides C, N, P, other fundamental elements for growth are S, K, Na, Fe, Mg, Ca and trace elements such as B, Cu, Mn, Zn, Mo, Co, V and Se. N, P and C are often limiting, and the oversupply is also no solution to the problem as this may lead to stress and reduced growth. Plotting the growth curve as function of time and nutrient concentration, 4 zones can be identified (Figure 1.4):

- A **deficient zone** (1) with low nutrient concentrations, growth increasing dramatically when nutrients are supplied;
- A **transition zone** (2) where the critical concentration is found, and this zone growth is little affected by the addition of more nutrients;
- An **adequate zone** (3) where no increase in growth is found with an increase in the supply of nutrients;

- A **toxic zone** (4) where an increase in the concentration of nutrients lead to reduce growth.

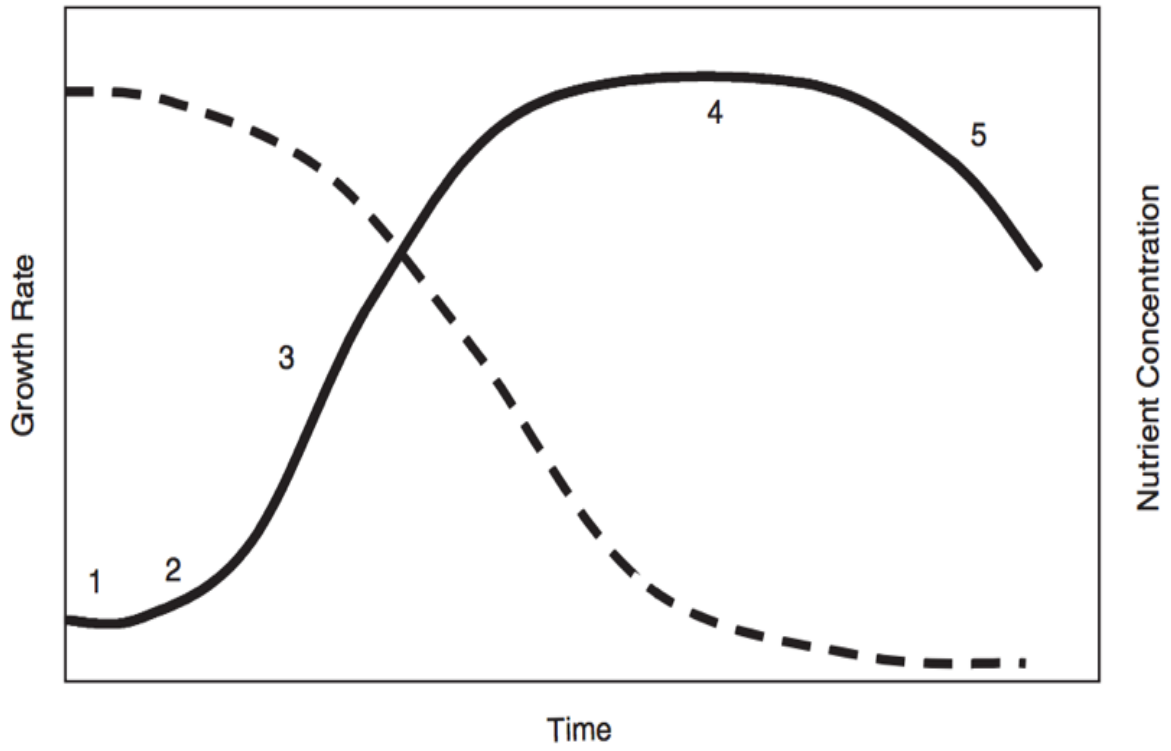

Figure 1.4 *Schematic growth curve in a batch culture. 1 lag phase, 2 exponential phase, 3 phase of linear growth, 4 stationary growth phase and 5 decline or death phase. (Richmond, 2004)*

For laboratory grown cultures the water used for making up the growth media is either single or double glass distilled water, membrane filtered water, or de-ionized water. The use of these treated waters is not possible for large-scale production purposed. In such cases either natural (surface or groundwater) or the available domestic waters are used. Residual chlorine may be present in domestic waters and this would necessitate an aging step before the water is used.
Usually culture media are formulated such that nutrients are supplied in excess to ensure that they never become the rate-limiting, at least if this is the purpose of the research.
The Table 1.1, on the next page, shows the composition of BG11 medium, widely used for microalgae growth of freshwater algae (Richmond, 2004). The BG11 medium, was used during this thesis work.

Table 1.1 *Recipes of BG11 growth medium used for growing algae. All concentrations are in g · l^{-1}, the quantities are for 1 litre of culture solution. (Richmond, 2004)*

Substance	Nutrient solution (g/l)
$NaNO_3$	1.5
$K_2HPO_4 \cdot 3H_2O$	0.04
$MgSO_4 \cdot 7H_2O$	0.075
$CaCl_2 \cdot 2H_2O$	0.036
Citric acid	0.006
Fe-Ammonium citrate	0.006
EDTA, 2Na-Mg salt	0.001
Na_2CO_3	0.02
H_3BO_4 (μg l^{-1})	2.86
$MnCl_2 \cdot 4H_2O$ (μg l^{-1})	1.81
$ZnSO_4 \cdot 7H_2O$ (μg l^{-1})	0.222
$NaMoO_4 \cdot 2H_2O$ (μg l^{-1})	0.391
$CuSO_4 \cdot 5H_2O$ (μg l^{-1})	0.079
$Co(NO_3)_2 \cdot 6H_2O$ (μg l^{-1})	0.0494
Adjust final pH	7.8

1.1.3 Growth phases

In unicellular microalgae, the cell size generally doubles and then the cell divides into two daughter cells, which will then increase in size. The cell cycle in eukaryotic microalgae is divided into two consecutive phases: interphase and mitosis. During the interphase, the cell grows, and its cellular components multiply in number, so that each daughter call can receive a complete set of replicated DNA molecule and a sufficient number of organelles and components. Then follows the mitosis during which the nuclear division takes place. As mentioned in the previous paragraph, growth is strongly influenced by various factors such as the accumulation of toxic metabolites or a law nutrients concentration. In fact, the development of secondary metabolites is often appreciable in the growth phases. Finally, when the energy is no longer sufficient for the maintenance of the vital function of the cell, we witness the decline and death of the same. This phase can be accompanied by the formation of spores that survive in critical and unfavorable conditions and then "reborn" in better conditions, in order to guarantee the survival of the specie (Richmond, 2004). Microalgae growth in a batch culture can be described through four phases (Figure 1.4):

- **Lag phase** (1): this is a phase of latency where microalgae must acclimate to new conditions such as medium composition, light intensity, temperature, etc. This growth delay can also be caused by the presence of dead cells in the initial inoculum. This

period of physiological acclimatization is closely linked to the phases of growth of the pre-inoculum and to the new phases of growth of the inoculum.

- **Exponential phase** (3): during this second phase, the cell density increases as a function of time according to a logarithmic function. The growth rate is always positive in the considered period of time and is dependent on the concentration of nutrients in the culture medium, the intensity of the light, pH and temperature. One factor to keep in mind is the shading (shadow caused by the increase in cell density within the growth space), which is minimal in the first part of the exponential phase**.** The time required to double the number of cells is defined doubling time (t_d), or generation time. It is the time necessary for microalgae to grow and produce a new generation of cells. The number of cells in an exponentially growing microbial culture could be mathematically described as follows:

$$2^0 N_0 \rightarrow 2^1 N_0 \rightarrow 2^2 N_0 \rightarrow 2^3 N_0 \rightarrow 2^n N_0 \quad (1.4)$$

N_0= Initial number of cells
n = Number of doublings (generation)

Number of doublings (n) at time interval t, is determined by the relation t/t_d. Thus, the number of cells (N_t) in an exponentially growing culture after being incubated for some time t, can be estimated:

$$N_t = N_0 2^n = N_0 2^{t/t_d} \quad (1.5)$$

$$N_t / N_0 = 2^{t/t_d} \quad (1.6)$$

$$\ln(N_t/N_0) = (\ln 2)\, t/t_d \quad (1.7)$$

During the exponential growth phase, the growth rate of the cells is proportional to the biomass of the cells. Since biomass generally can be measured more accurately than the number of cells, the basic microbial growth equations are often expressed in terms of mass. Hence, the Equation 1.7 can be modified, by assuming the biomass concentration at time 0 (initial) and time t as X_o and X_t, respectively:

$$\ln(X_t/X_0)/t = 0.693/t_d \quad (1.8)$$

$$d(\ln X)/dt = 0.693/t_d \quad (1.9)$$

$$d(\ln X)/dX \cdot dX/dt = 0.693/t_d \quad (1.10)$$

$$1/X \cdot dX/dt = 0.693/t_d \quad (1.11)$$

$$\mu = 0.693/t_d \quad (1.12)$$

Where μ represents the specific growth rate (d^{-1}) of the culture. It defines the fraction of increase in biomass over a unit time, i.e. an increase of certain g-biomass from every g of existing biomass per day. Specific growth rate represents the average growth rate of all cells present in a culture, but not necessarily the maximum specific growth rate of the individual cells, as most microbial cultures divide asynchronously.

- **Stationary phase** (4): The cell growth rate in this phase is very slow or even zero, usually corresponds to high cell concentration. Nourishing the nutrients in a balanced way, culture can be maintained at this stage.

- **Death phase** (5): usually this phase manifests itself when culture reaches a high cell concentration, in this case the nutrients are limiting, and this entails the death of the cultivated species (Lee, 2016).

1.1.4 Microalgae cultivation technologies

Algal cultures in a controlled environmental have been considered of strategic importance for the production of biomasses of various uses. The most recent frontier of algae culture aims to obtain large quantities of vegetable raw material to extract oils and substances with high nutritional value. In order to maximize the yields of the industrial plants destined to algal cultures, great attention was paid to the management of the optimal growth parameters in cultivation. The most studied parameters were the photoperiod, the quality of the light radiation, the temperature, the contribution of micro and macronutrients that can more stimulate the production of oils. The cultivation of unicellular algae biomass in a controlled environmental is part of the aquaculture activities of aquatic organisms. The protocols for the production of algae biomass are numerous and different among themselves for the system used, for the size, for the chemical-physical parameters and for the composition of the culture medium. The algal biomass cultures are essentially divided into two categories: indoor and outdoor. The indoor cultures are placed inside closed structures where it is possible to control all the growth parameters including the light radiation. This implies higher production costs but a higher yield thanks to the tighten internal control. Outdoor systems are logically cheaper thanks to the solar light intensity, but on the other side they are less controllable. The systems can also be divided into open or closed, the first use as environmental culture large tanks, canals, ponds or units with low water circulation, in the form of panels or circuits, made of polycarbonate pipes with forced circulation. The closed culture systems, also called photobioreactors, use large polyethylene bags or photobioreactors, cylindrical, helical annular and panel, to which radial energy is provided semi-continually or continually. Therefore, in the choice of the culture system we must consider various factors such as the physiological needs

of the algae, the quality of the products to be obtained and the economic aspect (Di Martino and Stancanelli, 2015).
The most widespread microalgae cultivation technologies will now be briefly described:

- **Open Ponds** (Figure 1.5). Open Ponds culture is cheaper than culture in closed photobioreactors and are the simplest cultivation systems used for large scale microalgae production, but it is limited to a relatively small number of algae species. Furthermore, commercial outdoor cultivation is generally restricted to tropical and subtropical zones in regions of low rainfall and low cloud cover. This type of system differs in shape, size, building materials and mixing equipment. Small ponds are more expensive to build per unit area than large ponds**,** the size affects water circulation, which in turn affects the design and operating costs. The final product destination affects pond choice: if the biomass is used for human consumption, the system must be capable of "cleaner" production on the contrary if the biomass is used for animal feed or energy a very high level of cleanliness is not required (Borowitzka, 2005).

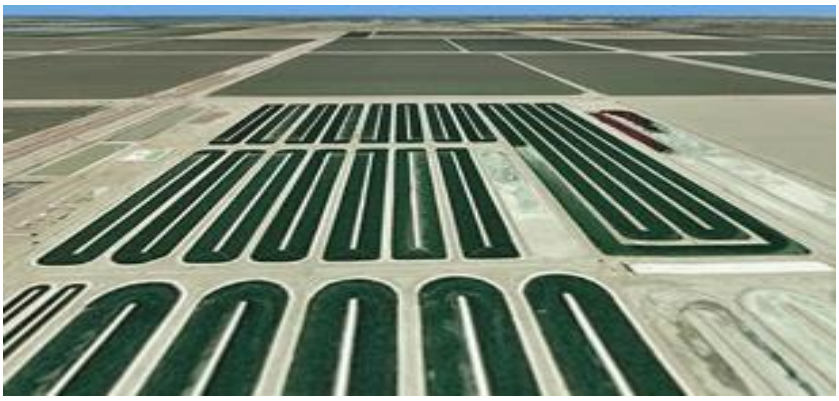

Figure 1.5 *Open Ponds. (http://www.algaedetective.com)*

- **Closed Photobioreactors (PBRs)** (Figure 1.6). This type of systems is characterized by the regulation and control of nearly all biotechnologically important parameters as well as by the following fundamental benefits: a reduced contamination risk, no CO_2 losses, reproducible cultivation conditions, controllable hydrodynamics and temperature, and flexible technical design. Closed photobioreactors are currently tested for microalgae mass cultures in the following configurations: tubular system (bags, plastic, glass), flattened, plate-type system and ultrathin immobilized configurations. Thanks to the above-mentioned benefits, this type of reactors allows to obtain high production efficiency, but the maintenance of the entire production system proves to be

expansive. This problem still limits the cost-effective production of microalgae biomass on large scale.

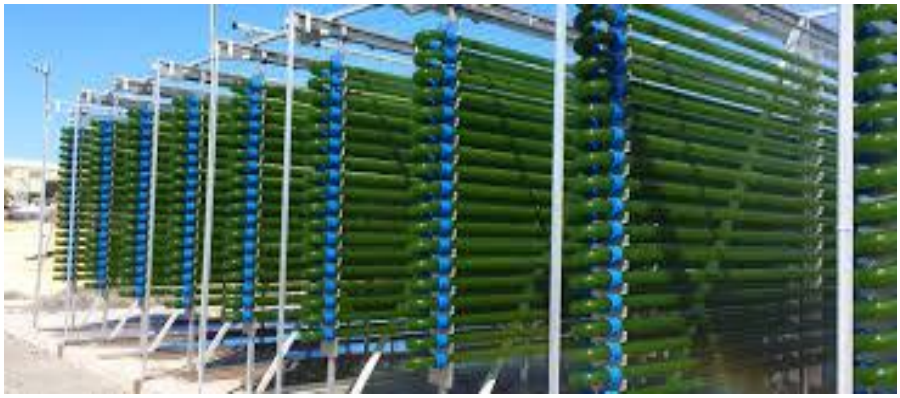

Figure 1.6 *Closed Photobioreactors PBRs. (http://www.variconaqua.com)*

The high uncertainly on the practicability of the cultivation at large scale microalgae cultivation requires continuous technological improvements and constant research. On this front, many researchers are engaged in the optimization of production processes to make this type of cultivation economically more advantageous.

1.2 Photosynthesis

Photosynthesis depicts a unique process of sunlight energy conversion. In this process, inorganic compounds and light energy are converted to organic matter by photoautotrophs (microalgae belong to this group). Virtually, all form of life on Earth depend directly or indirectly on photosynthesis as a source of energy for their metabolism and growth. This photosynthetic apparatus is organised in special organelles (Figure 1.7), the chloroplasts, which contain alternating layers of lipoprotein membranes (the thylakoids) and aqueous phases (the stroma) (Staehelin and Arntzen, 1986). All the chlorophyll and the photosynthetic reactions are located and take place in the thylakoid membranes and in most algal strains, the thylakoids are organised in pairs or stacks of three.

The thylakoid membrane contains five major complexes: light-harvesting antennae, photosystem II (PSII) and photosystem I (PSI) both containing a reaction centre, cytochrome b_6/f and ATP synthase, which maintain photosynthetic electron transport and photophosphorylation.

Carbon reduction reactions, which are catalysed by hydro soluble enzymes, take place in the stroma, the chloroplast region surrounding the thylakoids.

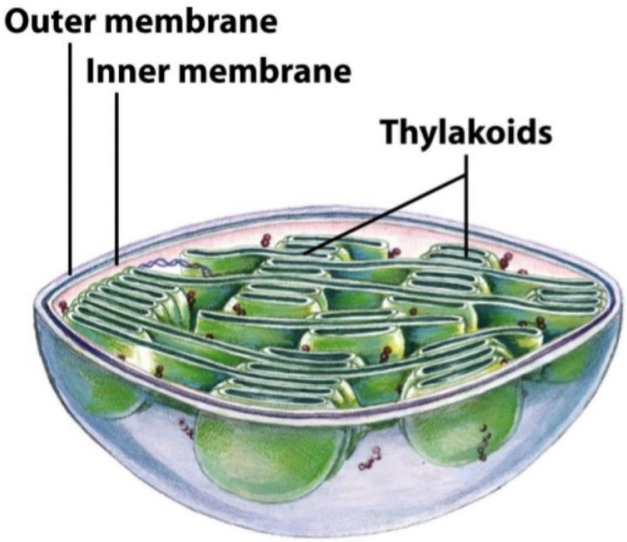

Figure 1.7 *Chloroplast, schematic diagram. (Nelson, 2006)*

Photosynthesis can be expressed as a redox reaction driven by light energy, in which CO_2 and water are converted to carbohydrates and oxygen. The conversion is traditionally divided into two stages, the so-called light reactions and dark reactions (Figure 1.8). In the light reactions, which are legate on photosynthetic membranes, the light energy is converted to chemical energy supplying a biochemical reductant $NADPH_2$ and a high energy compound, ATP. In the other reactions, the dark reactions that take place in the stroma, $NADPH_2$ and ATP are used in the sequential biochemical reduction of CO_2 to carbohydrates (Masojìdek *et al.,* 2004). The overall equation photosynthesis in vascular plants describes an oxidation-reduction reaction in which H_2O donates electrons (as hydrogen) for the reduction of CO_2 to carbohydrate (CH_2O):

$$CO_2+H_2O\rightarrow O_2+(CH_2O) \qquad (1.13)$$

The conversion of CO_2 to carbohydrate or other compounds, takes place in four distinct phases, these phases are called Calvin-Benson cycle:

1. **Carboxylation:** in this phase, CO_2 is added to the 5-carbon sugar (Ribulose phosphate) and forms two molecules of phosphoglycerate (6-carbon). The Rubisco enzyme catalyses this phase.

2. **Reduction**: the phosphoglycerate is convert in 3-carbon products in two steps, in first with the use of ATP and secondly with the use of $NADPH_2$.

3. **Regeneration**: Ribulose phosphate is regenerated for subsequent CO_2 fixation; this phase is completed by the action of the transketolase and aldolase enzymes.

4. **Production**: the main end products are carbohydrates but there are also fatty acid, amino acids and organic acid. The variety of the formed products depends on different conditions such as light intensity, nutrition and CO2 and O2 concentrations (Nelson, 2006).

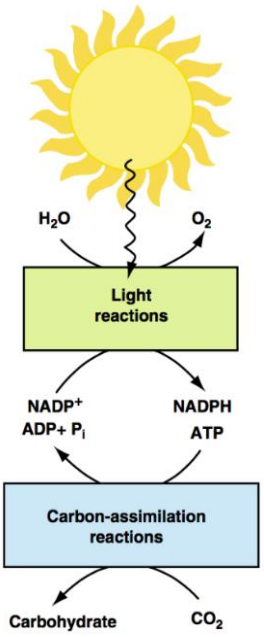

Figure 1.8 *In the light reactions generate NADPH and ATP at the expense of solar energy, in the dark reactions, these products are used in the carbon-assimilation reactions, to reduce CO2 to form carbohydrate. (Nelson, 2006.)*

The mechanisms of regulation of the photosynthetic apparatus will now be introduced, thus offering a more general panoramic approach and anticipating the phenomenon of chlorophyll fluorescence, a fundamental part of this work thesis.

The light energy is harvested by organic pigments that are contained in all photosynthetic organism, these pigments can be chlorophylls (Chl), carotenoids or phycobilins. All the pigment molecules in a photosystem can absorb light (Figure 1.9), but only few chlorophyll molecules associated with the photochemical reaction centre are specialized to transduce light into chemical energy.

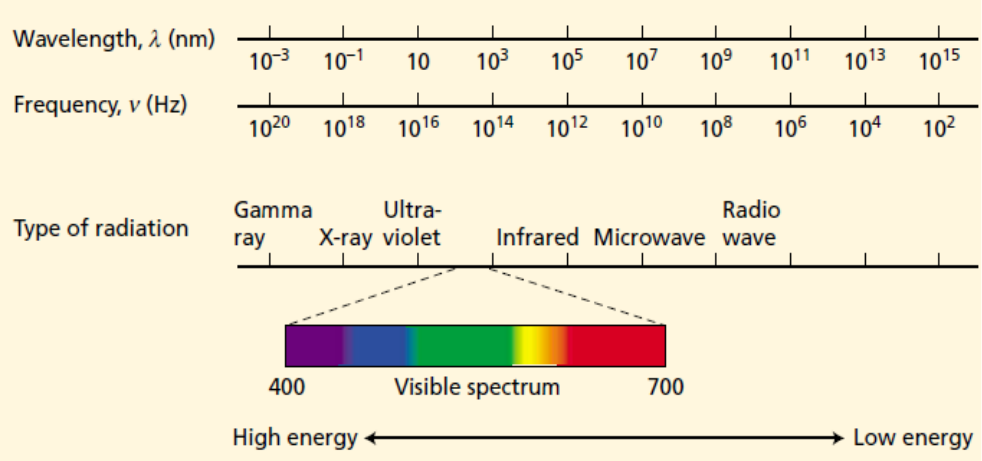

Figure 1.9 *Electromagnetic spectrum. Wavelength (λ) and frequency (ν) are inversely related. The visible region extends from about 400 nm (violet) to about 700 nm (red). (Taiz and Zeiger, 2010)*

Light is also a particle, which we call photon, and each photon contains an amount of energy that is called a quantum. The sunlight is like a rain of photons of different frequencies (ν) and the energy (E) of a photon depends on the frequency of the light according to Planck's law:

$$E = h \cdot \nu \tag{1.14}$$

where h is Planck's constants (6.626×10^{-34}Js).

Chlorophyll appears green because it absorbs light mainly in the red and blue parts of spectrum, so only some of the light enriched in green wavelengths about 550 nm is reflected. The absorption of light is described by Equation:

$$Chl + h\nu \rightarrow Chl^{*} \tag{1.15}$$

Where, *Chl* represents chlorophyll at the lowest-energy state, $h \cdot \nu$ represents a photon and Chl^{*} is the chlorophyll at the higher-energy state, or excited state.

Observing the Figure 1.10, we can see how the distribution of electrons in the excited molecule is somewhat different from the distribution in the ground-state molecule. Absorption of blue light excites the chlorophyll to a higher energy state than absorption of red light because the energy of photons is higher when their λ wavelength is shorter. Chlorophyll in the higher excited state is highly unstable and very rapidly gives up some of its energy to the surroundings as heat, and enters the lowest excited state, where it can be stable for a maximum of several nanoseconds (10^{-9} s), by reason of this strong instability any process that captures its energy must be extremely fast.

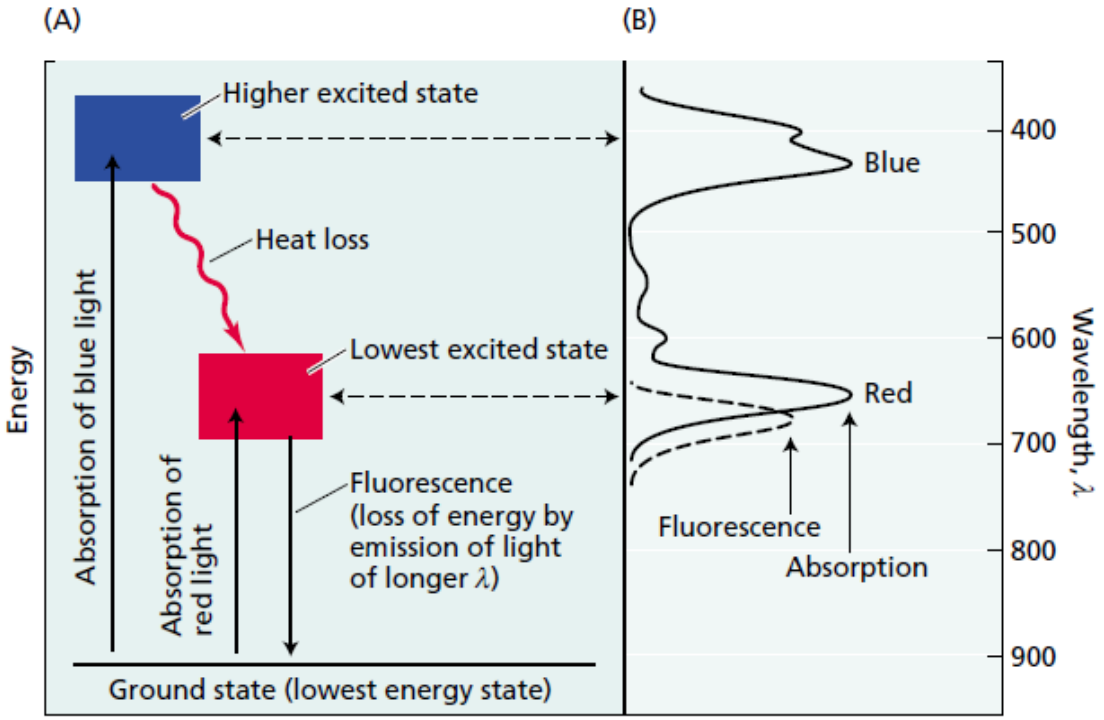

Figure 1.10 *Light absorption and emission by chlorophyll. (A) Energy level diagram. (B) Spectra of absorption and fluorescence. (Taiz and Zeiger, 2010)*

In the lowest excited state, the excited chlorophyll has three alternative pathways for disposing of its available energy:

1. **Photochemical**: the energy of excited state is transferred to the reaction centre, thus allowing the photochemical reactions. These reactions are among the faster chemical reactions, this speed is essential for the photochemical process to compete with the other possible reactions of the excited state.

2. **Heat**: the chlorophyll can return to its basal state, converting the excitation energy in form of heat, without emitting photons.

3. **Fluorescence**: the excited chlorophyll can emit a photon and return to its basal state; this process is called fluorescence. The wavelength of fluorescence is always longer than that of absorption at the same electronic state, since a part of the excitation energy is converted into heat before the photon is emitted. The chlorophylls are fluorescent in the red region of the spectrum, see Figure 1.11 (Taiz and Zeiger, 2010).

Figure 1.11 *False colour image shows the difference in FLUORESCENCE that specific cameras observe during the scans. (https://cahnrs.wsu.edu)*

In the paragraph §2.3.4 we will deepen the concept of chlorophyll fluorescence, process that is of fundamental importance for this entire study. We will talk about the process from a chemical-physical point of view and about the appropriate instrument used for its detection.

1.3 Industrial applications of microalgae

This section aims to provide the reader with a brief overview of the main applications of microalgae. Even if the application for energetic purposes is the best known and studied in reality there are other growing markets that utilize this raw material from high nutritional properties. In fact, it ranges from the production of biofuels to the pharmaceutical and cosmetic industries, from the production of food additives for human purposes to animal feed.

We want to introduce some notes about the field of biofuels and its development. In these last years, ecologically and politically sustainable development models have been investigated due to the need to meet the high energy demand of an increasing word population, and also to reduce greenhouse gas emission and the effects of global warming at the same time. In 2013, world demand of diesel fuel reached nearly 26.1 thousand barrels per day and it is expected to be 36.1 thousand barrels per day in 2040 (OPEC, 2015). Recent studies have shown how the production of biodiesel from microalgae is a promising way to obtain both a high quality and environmentally-friendly diesel fuel. Microalgae can accumulate various types of high-energy compounds, such fatty acids and triacylglycerols, which are the principal components for biodiesel production (Leite *et al.*, 2013).

After a period of growth that allows the development of microalgae, the biomass is usually separated through centrifugation, filtration techniques or flotation. Once this raw material is obtained, different refining processes can be carried out, according to the final product to be

obtained. Through a process of extraction such as transesterification biodiesel can be obtained, or through the use of supercritical fluids such as CO_2, high value compounds can be obtained. In addition, gasification, combustion and fermentation processes make it possible to obtain, bio-plastic, ethanol, bio-hydrogen and green energy (Patel *et al*., 2017).

Precious co-products, such as proteins and pigments, can be obtained from microalgae through the modulation of biomass composition by modifying the nutritional requirements, growth conditions and process technologies (Bona *et al.*, 2014) based on the use desired final use. As regard the nutraceutical sector, a few compounds synthesized by microalgae have indeed proven to possess anti-inflammatory, antiviral, antimicrobial, and antitumoral features; astaxanthin, a known antioxidant produces by *Haematococcus pluvialis*, is an illustrative example with important anti-inflammatory and antitumoral roles (Guendales *et al*., 2010).

Hereafter in Table 1.2, some species of microalgae and their lipid content will be listed.

Table 1.2 *Lipid content and productivity of freshwater and marine species. (Mata et al., 2010)*

Marine and freshwater microalgae species	Lipid content (% dry weight biomass)	Lipid productivity (mg/l/day)
Chlorella protothecoides	14.6-57.8	121.4
Chlorella vulgaris	5.0-58.0	11.2-40.0
Chlorella	18.0-57.0	18.7
Dunaliella salina	6.0-25.0	116.0
Dunaliella primolecta	23.1	-
Euglena gracilis	14.0-20.0	-
Haematococcus pluvialis	25.0	-
Isochrysis galbana	7.0-40.0	-
Monodus subterraneus	16.0	-
Nannochloropsis oculate	22.7-29.7	84.0-142.0
Nannochloropsis sp.	12.0-53.0	37.6-90.0
Pavlova salina	30.9	49.4
Scenedesmus obliquus	11.0-55.0	-
Scenedesmus quadricauda	1.9-18.4	35.1
Spirulina platensis	4.0-16.6	-
Tetraselmis suecica	8.5-23.0	43.4

Another microalgae now renowned for its nutritional properties is *Spirulina* (Figure 1.12), which has now become common in many food supplements. It contains phycocyanin a pigment with antihypertensive effect useful in lowering blood pressure, *Spirulina* benefits have also been shown to prevent atherosclerosis and reduce elevate blood cholesterol levels (Cheong and Kim, 2010). It can also curb hunger and overweight people seem to benefit the most, moreover, compared to placebo trials, this microalgae is effective in reducing itching, nasal discharge, nasal congestion and sneezing in case of allergenic rhinitis (Saying *et al*., 2013).

Figure 1.12 *Spirulina. (http://www.stylecraze.com)*

The application of microalgae in cosmeceutical products have recently received more attention in the treatment of skin problems, such as aging, tanning and pigment disorders. The name "cosmeceutical" is derived from cosmetics and pharmaceutical, indicating that a specific product contains active ingredients. These active ingredients are ω-3 fatty acids, essential amino acids, vitamins A, B, C and E, sulphated polysaccharides, tyrosinase inhibitors and phlorotannins, now widely recognized for their antioxidant properties and skin protective effects (Noel Vinay and Se-Kwon 2013).

Finally, it can be mentioned the possibility of coupling the microalgae production process to industrial CO_2 mitigation and wastewater treatments to finally recycle carbon, nitrogen and phosphorous. Microalgae can sequester carbon dioxide thereby reducing greenhouse gases (Ho *et al*., 2011) and do not compete with food production or deplete soil nutrients.

The fields of application (Figure 1.13) are therefore innumerable and multi-faceted, united by constant research and the continuous development of improvements.

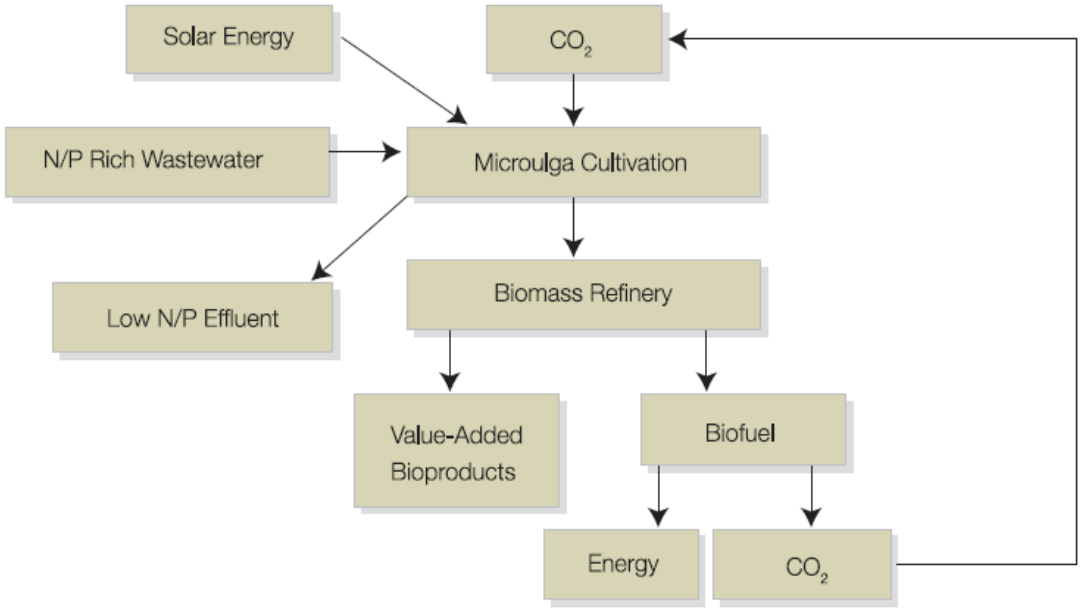

Figure 1.13 *A conceptual microalgal system for combined biofuels production, CO_2 bio-mitigation, and N/P removal from wastewater. Inputs: carbon source, CO_2, nitrogen and phosphorus sources, N/P rich wastewater; energy source, solar energy. (http://www.climatetechwiki.org)*

1.4 Objective of this work

Reading the previous paragraph, we can easily understand how microalgae represent a promising field for various industrial sectors, ranging from sustainable production of biofuels to the extraction of high value-added products. To make these microorganisms "attractive" to the industrial sectors, their growth process must be further optimized. Since the microalgae growth is directly dependent by huge numbers of variables (e.g. light intensity, nutrients concentration and temperature), numerous and time-consuming experiments are required to assess their impact on the growth. For this reason, microscale technologies are emerging as a valuable tool to improve data production and accordingly to speed up the optimization process, while maintaining a high experimental reliability (Perin *et al*., 2016).

Since this kind of microfluidic devices does not allows an optimal carbon dioxide supply from the atmosphere, the first aim of this work consists on the design of an efficient CO_2 supply system thus granting a non-limiting condition for the microalgae growth. In this study, microalga *Scenedesmus obliquus* is chosen as a reference species to assess the effectiveness of the proposed supply protocol.

The microalgae growth is evaluated *in vivo* by measuring the fluorescence emitted by the chlorophyll contained in the algae, the correlation between cell concentration and fluorescence was obtained through an appropriate calibration line.

Chapter 2

Materials and methods

In this chapter, the general concepts concerning the microfluidics technology (science) and the micro-photobioreactor (micro-PBR) will be presented. Secondly, the equipment, the materials and the methods adopted to monitoring the microalgae growth will be described.

2.1 Microfluidics

Microfluidics is the science and engineering of system in which fluid behaviour differs from conventional flow theory primarily due to the small length scale of the system.

Microfluidics is a recent research field that concerns the manipulation and the transport of small amounts of liquid (1pl – 1ml) in channels of micrometric dimension. Microfluidics can be considered both a science and a technology depending on whether it is a study of microfluidic behaviour or a study with a microfluidic device. The Figure 2.1 shows the volume scale and length scale of different microfluidic devices.

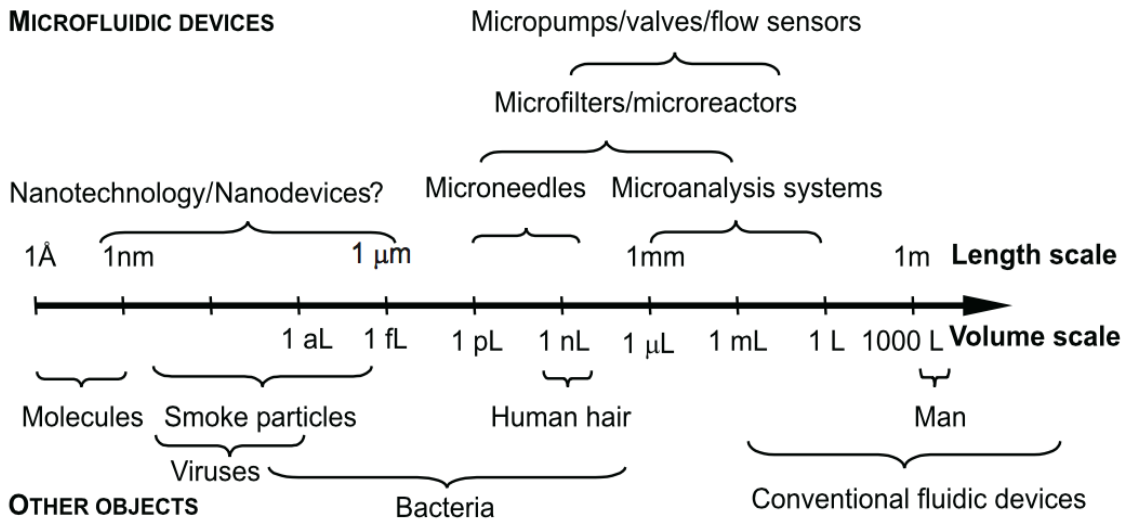

Figure 2.1 *Size characteristics of microfluidic devices. (Nguyen and Wereley, 2006)*

Fluids behave very differently on the micrometric scale than they do in a macrometric scale: these unique features are the key for new scientific experiments and innovations.
Microfluidics has the potential to influence many areas of interest, from chemical synthesis and biological analysis to optics and information technology. In any case, this science and technology is in continuous development. In each field of interest, it is necessary to identify the purpose of the research and find the most appropriate solution. Often various problems need to be addressed and features such as imagination and ingenuity are necessary. In any case, the advantages in using this technology are countless and some of them will be listed below (Whitesides, 2006):

- ability of using small quantities of samples and reagents and carry out separations and detections with high resolution and sensitivity;
- faster analyses due to the shorter reactions and/or separation times;
- low cost and global cost reduction for analysis;
- formats more compact and more versatile;
- accurate measurement, microfluidics allowing to increase the measurement resolution in given applications;
- enhanced temperature control;
- easier automation and parallelization;
- ability to obtain many data in a single experiment.

The field of microfluidics derives from the microanalytical methods and has four parents: molecular analysis, biodefence, molecular biology and microelectronics.
Thanks to the development of increasingly advances technologies in the manufacturing field, in recent decades we have witnessed a growing interest in the sector of microfluidic devices.
Over the 80s, a new sort of devices called Micro Electro Mechanical System (MEMS) emerged, allowing industrial applications. In the 90s, researchers spent a lot of time investigating the applications of MEMS in biology, chemistry and biomedical fields in order to allow the control of liquids in microchannels, in the late 90s, the use of soft-lithography allowed the production of chip microfluidics devices by using moldings of polymer. In the early 2000s, technologies based on molding microchannels in polymers like PDMS encountered a great expansion and a large number of laboratories were able to conduct microfluidic research (ELVESYS R&D team, 2018a).

2.1.1 Microfluidic device

In order to consider a device microfluidic, at least one dimension of the channel must be in the range of micrometers. These devices are very adaptable and allow the integration of lab

routines in one single chip (lab-on-a-chip). Lab-on-a-chip is a term used to describe a device where multiple actions are carried out, comparable to those performed inside a laboratory (sampling, trapping and sorting, treatment and analysis). Although the concept of lab-on-a-chip has now become widespread, it must be noted that these chips have not yet invaded the market but are only used in research. The main reason for this delay lies in the nature of microfluidics: in fact, while the possibility to produce these chips is known, the accurate control of flows and volumes of liquids on micro-nano-metric scale is the major problem. Indeed, move or mix liquids in channels of a few microns diameter involves a series of physical parameters that escape our macroscopic vision. The flows in these conditions are usually laminar and due to the high ratio area/volume, the interfaces characteristic became relevant. In microfluidics systems, capillary forces are more important than gravitational force, this aspect has two different consequences: the first is that the channels characteristics must be controlled, but secondly it possible to have a greater manipulation of liquids.

The microfluidics device consists of a single chip ranging from a few millimetres to a few square centimetres. A microfluidic chip is a pattern of microchannels, modelled or engraved. This network of microchannels incorporated into the microfluidic chip is linked to the macro-environmental by several holes of different dimensions hollowed out through the chip, it is through these pathways that fluids are injected into and evacuated from the microfluidic chip.

Microfluidic systems manipulated and control fluids that are geometrically constrained within environments having internal dimensions, or hydrodynamic diameters, on a scale of micrometres. To accurate manage fluids inside the microchannels, specific systems are required (pressure regulators, valves, syringe pumps).

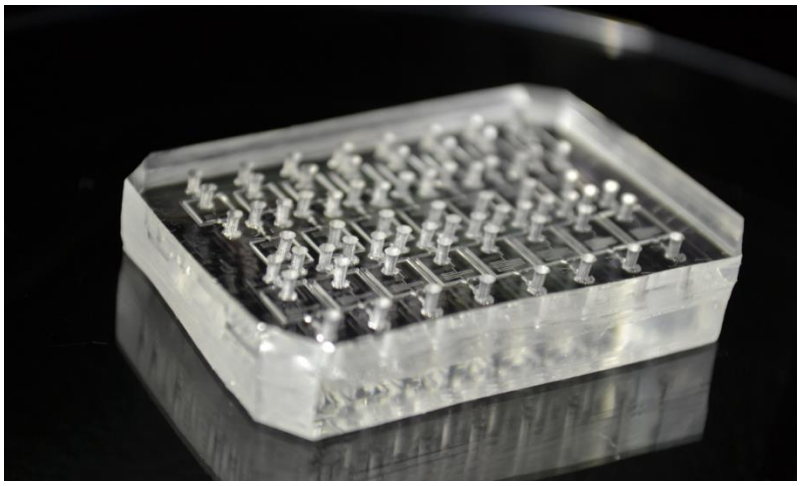

Figure 2.2 *Microfluidic device in PDMS. (http://www.ntnu.edu/microfluidics)*

The use of diverse materials for microfluidics chips such as polymers (e.g. PDMS), ceramics (e.g. glass), semiconductors (e.g. silicon) and metal is currently possible because of the

development of specific processes: deposition and electro-deposition, etching, bonding, injection molding, embossing, soft-lithography and stereolithography (especially with PDMS). Access to these new materials has allowed the design of chips with new features like specific optical characteristics, biological or chemical compatibility, faster prototyping or lower production costs. The final choice depends on the application (ELVESYS R&D team, 2018b). Moreover, the possibility of automating the procedures related to the microfluidics chip control, is making this technology more and more interesting. The ability to automate the devices moves hand in hand with the development if increasingly sensitive and precise equipment.

2.2 Material and equipment

In this paragraph the methods and the main equipment necessary for the creation and operation of the microfluidic chip will be listed and described. First the poly-di-methyl-siloxane (PDMS) will be panned, giving a brief overview of the materials and its advantages. In the last part experimental setup will be explained.

2.2.1 PDMS

Poly-di-methyl-siloxane called PDMS or dimethicone is a polymer widely used for the fabrication and prototyping of microfluidic chips. It is a mineral inorganic polymer with a structure containing carbon and silicon, of the siloxane family. Apart from microfluidics, it is used as a food additive (E900), in shampoos, and as an antifoaming agent in beverages or in lubricating oils.

The PDMS empirical formula is $(C_2H_6OSi)_n$ and its fragmented formula is $CH_3[Si(CH_3)_2O]_nSi(CH_3)_3$ (Figure 2.3), industrial synthesis can being from dimethyldichlorosilane and water. Depending on the size of monomers chain, the non-cross-linked PDMS may be almost liquid (low *n*) or semi-solid (high *n*). The siloxane bonds (Si-O) result in a flexible polymer chain with a high level of viscoelasticity.

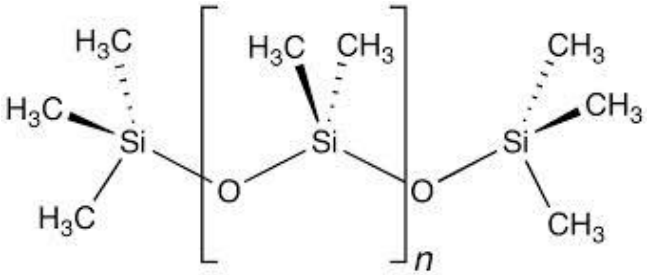

Figure 2.3 *PDMS structure formula. (ELVESYR R&D team, 2018c)*

For the fabrication of microfluidic devices (replica molding), PDMS liquid at ambient temperature, mixed with a cross-linking agent is poured into a microstructured mold and heated to obtain an elastomeric replica of the mold (PDMS cross-linked).
After polymerization and cross-linking, slid PDMS will present an external hydrophobic surface. Polar solvents, such as water, struggle to wet the PDMS and this leads to the adsorption of hydrophobic contaminants from water on PDMS surface (ELVESYS R&D team, 2018c). To overcome this specific problem, the chip is usually subject to plasma treatment which will be explained later in paragraph §2.2.4
Finally, it is necessary highlight that PDMS is an excellent material for the fabrication of microchannels system for use with biological sample in aqueous solution for a number of reason:

- feature on the micron scale can be reproduced with high fidelity in PDMS by replica molding;
- it is optically transparent down 280 nm so it can be used for a number of detection schemes (e.g., UV/V is absorbance and fluorescence);
- it cures at low temperatures;
- it is nontoxic; and devices made from it can be implanted in vivo;
- it can be deformed reversibly;
- it can seal reversibly to itself and a range of other materials by making molecular (van der Waals) contact with the surface, or it can seal irreversibly after exposure to an air plasma by formation of covalent bonds;
- its surface chemistry can be controlled by reasonably well-developed techniques;
- it is elastomeric, it will conform to smooth, nonplanar surfaces, and it releases from delicate features of a mold without damaging them or itself (McDonald et al., 2000).

For this series of advantages, the micro-PBR manufacture in PDMS turns out to be the optimum choice, the PDMS used is the Sylgard, 184 (Dow Corning, USA).

2.2.2 Microchip production

The fabrication of microfluidic devices adopted in this work is divided into several step, first the platform is designed with the aid of 3D CAD software then the mold (WATERSHED XC 11122(by Proto Labs)) was produced via stereolithography (SL) rapid prototyping. This technique is an excellent choice for project designed that require the production of very accurate and finely detailed parts. Stereolithography uses an ultraviolet laser focused to small point to draw on the surface of liquid thermoset resin. Where it draws, the liquid turns solid. This is repeated in thousands of thin layers until a final part is formed (Proto Labs, 2018).

Finally, the final device was replica-molded in PDMS. The pre-polymer Sylgard 184 (Dow Corning, USA) is mixed with a cross-linking agent in a ratio of 10:1 (w/w) and then poured onto the mold and degassed in a desiccator to eliminate air bubbles.

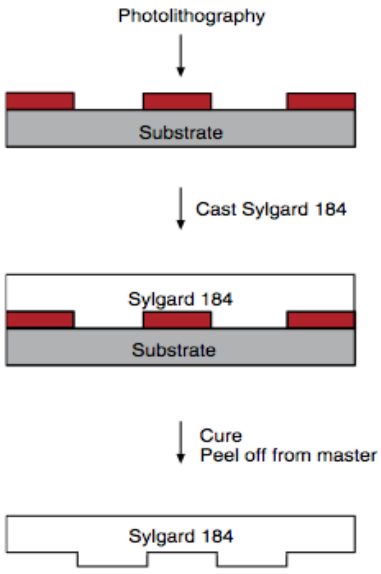

Figure 2.4 *Schematic illustration of the procedures for fabricating chip in PDMS. (Qin et al., 2010)*

During the chip and layer (necessary to guarantee sterility and avoid evaporation) manufacturing phases, particular attention must be paid to the two reagents mixing, the pre-polymer Sylgard 184 (Dow Corning, USA) and the cross-linking agent. The mixing must be perfect in order to allow a homogeneous polymerization and to guarantee that the final micro device complies with all structural and material standards. Another point on which to focus is the degassing procedure, in this phase it is necessary to ensure the total disappearance of air bubbles in the polymer before it is poured into the mold. The polymer degassing phase is a long procedure but must be carried out in a rigorous way. Once the PDMS is poured into the mold, it is better to make sure that no bubbles have been created, degassing it for a few minutes. After curing at 50° for 3 h, the micro-PBR and the layer in PDMS are ready for use. The layer is punched (diameter 1.5 mm) in correspondence with the flow channels. The flow channels and the micro-channels in hydrophobic PDMS are difficult to wet with aqueous solutions, are prone to the adsorption of other hydrophobic species, and easily nucleate bubbles. Exposure to plasma oxidation, however, renders the surface hydrophilic because of the presence of silanol groups.

Plasma treatment of silicone surfaces is a useful way of increasing wettability and to improve adhesion. The plasma treatment includes physical bombardment by energetic particles and by

ultraviolet photons, and chemical reactions at or near the surface. The resulting four main effects, namely cleaning, ablation, crosslinking, and surface chemical modification, occur together in a complex synergy, which depends on many parameters controlled by the operator. In this thesis work it was decided to subject the chip to a short plasma treatment (30 s) before autoclaving, this allows the future removal of the layer from the micro-PBR and the possibility to take a sample (useful for analysis).

2.2.3 Syringe pump

As previously mentioned in §2.1.1, microfluidics devices need special equipment because the flow inside the channels must be precisely controlled. The conventional pumps can generate flow oscillation at low flow rates and long setting times. It is especially the case when there is an inadequate combination of syringe size and targeted flow rate, or when a low flow rate is used, the reason for this behavior is mechanical. The mechanical part of the device is responsible for these oscillations. In order to move the piston syringe, an electrical engine sets an endless screw in motion, on which the piston carriage is set. When the flow rate is low, it happens that the step-by-step operation of the electrical engine is perceptible because the syringe pump piston has to move very slowly to deliver the required flow rate (ELVESYS R&D team, 2018d).

In this thesis work it was used a Harvard Apparatus PHD ULTRA™ syringe pump, it is an excellent example of a microfluidic syringe pump that does not generate visible flow oscillations, even at low flow rates down to the picoliter/min. The pump can reach a minimum flow rate of 1.5 pl/min when using a 0.5 µl syringe. The accuracy of the PHD ULTRA™ is 0.25% with a reproducibility of +/- 0.005%. To achieve the performance required for microfluidic devices, this syringe pump uses a microprocessor-controlled small step angle stepper motor which drives a lead screw and pusher block. Advanced micro-stepping techniques are employed to further reduce the step angle to eliminate flow pulsation. The syringe pump produced 12 800 µsteps per one revolution of the pump lead screw and has a minimum pusher block travel rate of µm/min (ELVESYS R&D team, 2018e). The pump can be oriented vertically or horizontally for optimum experimental connectivity. The pump is equipped with an intuitive touch screen includes pre-programmed methods, for various fluidics applications. All programming is done on the pump interface, all without the use of a PC. The PHD ULTRA™ also has the possibility to be connected with a camera and a microscope. The feature is very useful as more microfluidic experiments require synchronization between several instrumentation.

Figure 2.5 *Harvard Apparatus PHD ULTRA™. (PHD ULTRA™ Syringe Pump Service User's Guide)*

To operate the PHD ULTRA™, the user defines all the required parameter for infusion or withdrawing liquids through a Pump Control Method. The syringe pump is available in three configurations designed for different operating environments and varying degrees of operational flexibility:

- Infuse Only
- Infuse/Withdraw
- Infuse/Withdraw Programmable

In our specific case, the choice was the Infuse/Withdraw configuration. This model supports infusion and withdraw operations at user-definable flow rates and with selectable target volumes or time values to control the total volume pumped for both the infusion and withdraw portions of procedure (Harvard Apparatus, 2018).
When the flow rates are changed, the device requires a setting time ranging from a few second to hours, this depends mainly on the elasticity of the system and how small the flow is. In any case, when the syringe pump is loaded, it must be ensured that the syringes are free of air bubbles.

2.3 Microalgae growth monitoring

This section is dedicated to the description of microalgae growth monitoring methods, in the first part we would introduce the most classic methods such as Optical Density, cell counting through Bürker Chamber and Dry Weight. The last part is reserved for the explanation of the chlorophyll fluorescence phenomenon and to its detection method using the PAM-IMAGING Fluorometer.

2.3.1 Optical Density

Estimation of the microalgal biomass concentration via optical density (OD) at 750 nm wavelength is a rapid and common approach. However, the accuracy of this method might be affected by wavelength, microorganism morphology and culture medium composition. Error between the actual value and the predicted value is always in accepted range for biomass measurement (Ding *et al.,* 2015). However, attention must be paid to the microalgae growth phases because only during the logarithmic growth phase cells number is related to optical density. When the culture reaches the stationary phases, OD increase while the number of cells remains constant (Sforza, 2012).

The instrumentation used to measure optical density is the double-beam spectrophotometer UV-500 UV- Visible (Spectronic Unicam) (Figure 2.6).

The purpose of this tool is to determine the amount of light at a specific wavelength absorbed by an analyte in a sample, therefore the analytical wavelength is chosen based on the absorbance characteristic of the analyte.

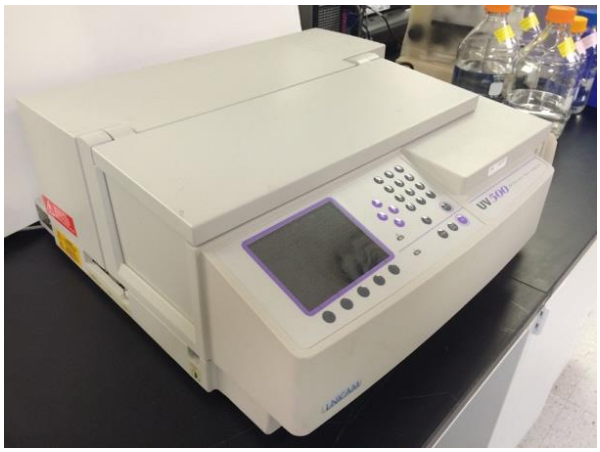

Figure 2.6 *Spectrophotometer UV-500 UV-Visible (Spectronic Unicam). (www.Labequip.com)*

The spectrophotometer consists of two lamps, one that covers the visible spectrum (930-300 nm) and one that emits a continuous spectrum below 400 nm (UV).

For the microalgae optical density measurements, a wavelength of 750 nm is chosen, at this specific wavelength the chlorophyll contained in the algae does not absorb photons. This allows us to say that the absorbance detected is due only to the light diffraction caused by the cells and the solid particles contained in the sample. These measures are not actually absorption measurement but light scattering measures, scattering is a phenomenon of interaction between matter, in this specific case cells, and light.

To detect the absorbance, the sample must be diluted appropriately so that the measurement is between a value of 0 and 1, because outside this range the linearity of the absorbance with respect to the cells concentration is not maintained. Before making the actual measurement, it is necessary to make a measure with blank sample, this sample is composed by algal culture medium, this test is necessary because the background noise of the instrument must be removed. After that procedure, it is possible to make an OD measurement, the number that appears on the display will be multiplied by the dilution factor in order to obtain the final result. This type of measurement is very useful to have a quick estimate of the pre-inoculum, in the initial phase of the experiment.

2.3.2 Bürker Chamber

Bürker chamber is a counting chamber serve to determine the number of particles per volume unit of a liquid. The particles in this case are microalgae and they are visually counted under a microscope. The Bürker chamber showed in Figure 2.7a has a spring clips and is a glass support measuring 7.5×3.5 cm size and 4 mm thick.

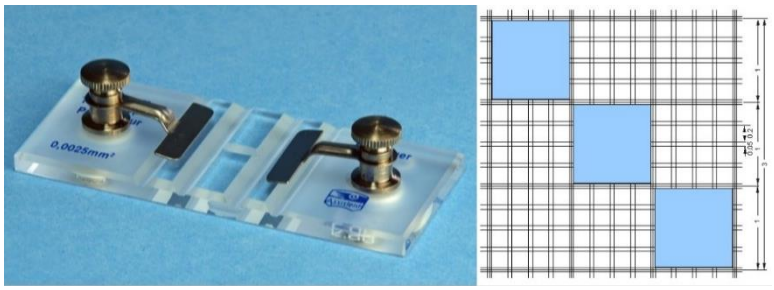

(a) **(b)**

Figure 2.7 *Bürker chamber and the reticulum*

The chamber is made up of two cells 0.1 mm deep, on which 9 squares 1×1 mm are engraved, divided by three continuous lines (reticulum). Each of these 9 squares is divided into 16 small squares by a double line. The count occurs on the 3 squares diagonally, as show in the Figure 2.7b, and the average is calculated. The cell count is carried out by taking a sample (2 ml) and diluting it by a factor between 5 and 50 depending on the estimated concentration. Each cell is loaded with 10 µl of the diluted sample it is now necessary to wait 5 minutes for the cells to settle on a single focal plane. Finally, we proceed with the count and the calculation of the cell concentration through the following formula:

$$cells/_{ml} = \left(\sum counted\ cells/_{3}\right) \cdot dilution \cdot 10^{4} \qquad (2.1)$$

The term 10^4 represents the volumetric factor which depends on the volume of the Bürker chamber (1/0.0001 ml). Also, in this case the measure also serves to identify the initial concentration of the pre-inoculum.

2.3.3 Dry Weight

The dry weight (DW) allows to determine the quantity of algae biomass per unit of volume. The procedure consists in taking 5 ml of sample which will be filtered through a Whatman NC 20 Membrane filter (0.2 μm pore diameter) placed over a vacuum flask, fixed with a Buchner steel funnel. The filter must first be weighed with a precision balance Atilon Acculab Sartorius Group (with a display precision of 0.0001g), after being placed in the oven for 20 minutes in order to eliminate humidity. After filtering the sample, the filter should be placed in the oven for 2 h at 100 °C. The filter taken gently from the oven is weighed (gross weight), to this the weight of the filter is subtracted, in this way we obtain the weight of the microalgae biomass (net weight), from which it is possible to calculate the culture concentration (g/l) in terms of DW with the following formula 2.2:

$$DW\ (g/l) = {(gross\ weight\text{-}net\ weight)\cdot 1000}\ /_{sample\ volume} \qquad (2.2)$$

2.3.4 Chlorophyll fluorescence and PAM-imaging Fluorometer

In this thesis work, it was necessary to apply a simple and non-invasive method able to evaluate the microalgae growth that allows an on-site evaluation of the same without compromising the experiment. The use of classical techniques such as OD, DW and cell counts with Bürker chamber implies the collection of quantities not negligible with respect to the adopted microfluidic system. Each well of the microphotobioreactor contains a volume of 20 μl, it is therefore impossible to take samples of quantities useful for the analysis and furthermore the sampling would definitively compromise the progress of the experiment. In the photosynthesis researches a functional and advantageous techniques is the *in vivo* measurement of chlorophyll fluorescence. Through the use of an instrument called fluorometer it is possible to measure fluorescence, which is directly related to algal growth, an increase in fluorescence indicates an increase in cell concentration, because the chlorophyll fluorescence reflects the activity of PSII (Murchie and Lawson, 2013). By a suitable calibration line, it is possible to quantitatively define microalgae growth (Perin *et al.*, 2016). After having previously introduced chlorophyll photosynthesis in section §1.2, chlorophyll fluorescence will now be introduced.

The possibility of quantifying the chlorophyll fluorescence directly reflects the performance of photochemical processes in PS II because the contribution of PS I emission in the total signal is usually neglected for practical purposes (we ignore emission from PSI largely because the signal does not make a significant contribution below 700 nm (Murchie and Lawson, 2013). The absorbed light energy can dissipate as heat (re-emitted) or can be used to excited chlorophyll molecules in PS II (drive photosynthesis) or alternatively re-emitted as fluorescence, in any case the amount of light energy absorbed is equal to the sum of the energy divided between these three different dissipation processes (see paragraph §1.2.1).
Each variation in photochemical process or in heat generate a variation in fluorescence. This allow a direct knowledge of energy contents in the PS II. In the dark phase all the reaction centres are "open" and the fluorescence in this state is minimal and is defined as F_0 or background fluorescence. Many instruments have the capacity to apply a weak far-red (FR) light to measure F_0 (typically a few seconds) (Murchie and Lawson, 2013). When the PS II are exposed to strong light pulses, the reaction centres undergo a charge separation and the electron is moved to the first electron acceptor Q_A.

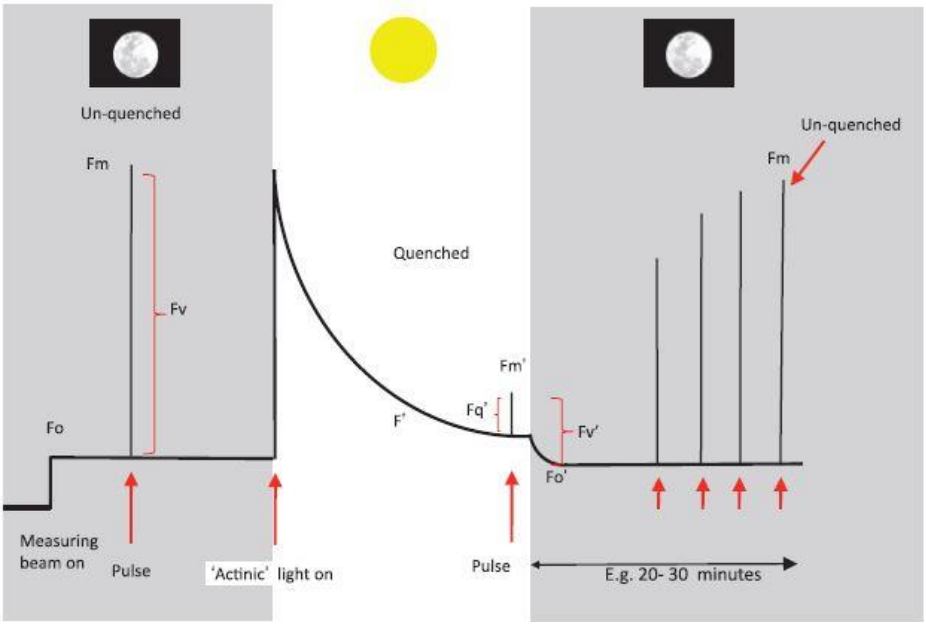

Figure 2.8 *A stylized fluorescence trace of a typical experimental using dark-adapted leaf material to measure photochemical and non-photochemical parameters. The Kautsky effect represent the complex fluorescence emission dynamics of chlorophyll and the photochemical yields of plants during the transition from a state adapted to darkness to a light adapted state. (Murchie and Lawson, 2013).*

Once Q_A is reduced, the reaction centres are defined as "closed" and the photochemistry is temporally blocked. Since the photochemistry is zero, the dissipation (heat) and fluorescence increase proportionally, and the maximum fluorescence value is defined as F_m. If a sufficiently strong actinic light is now applied, the yield of fluorescence increases proportionally with the

level of closure of PS II, in this sense the reaction centre acts as a fluorescence quencher. This phenomenon is called photochemical quenching q_P and can be calculated as $(F_m-F_t)/(F_m-F_0)$, where F_t is a steady-state yield of fluorescence. The value of q_p range from 0 to1 reflecting the relative level of Q_A oxidation. The difference between the maximum fluorescence F_m (all Q_A reduced) and minimum fluorescence F_0 (all Q_A oxidiser) is denoted as the variable fluorescence F_v. The ratio between variable fluorescence and maximum fluorescence F_v/F_m varies between 0.65 and 0.80 in green algae adapted to the dark. When the photosynthetic apparatus is exposed to light, a decrease in F_m is usually observed (lowered fluorescence in light phase F_m^L). This phenomenon is called non-photochemical quenching and represents an increase heat dissipation of excitation. The non-photochemical quenching is inversely related to photochemistry and it's a sort of safety valve protecting PS II reaction centres from damage by excess irradiance (Masojìdek *et al*., 2004).

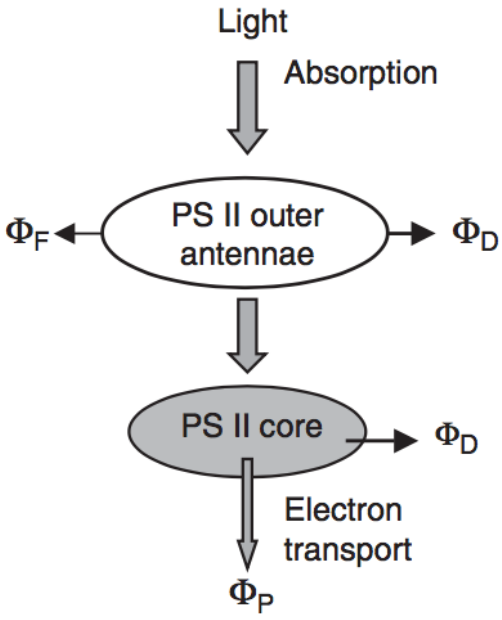

Figure 2.9 *Schematic representation of absorbed light energy distribution in the PS II complex between photochemistry Φ_P, fluorescence Φ_F and non-radiative dissipation Φ_D; the latter Φ_D can occur in the antennae as well as in the reaction centre. Φ_P, Φ_F, Φ_D represent the yield of photochemistry, fluorescence and non-radiative* dissipation, respectively. (Masojìdek et al., 2004)

The fluorescence parameters described above, and the relative calculations are shown in the Table 2.1.

Table 2.*1* *Parameters calculated from the chlorophyll fluorescence measurements; where F_0, F_v and F_m are respectively the background, variable and maximum fluorescence in the dark phase; while F_0^L, F_t and F_m^L represent the background, steady-state and maximum fluorescence in the light phase. (Masojìdek et al., 2004)*

Parameters	-	
Photochemical maximum yield PS II	F_v/F_m	$F_v/F_m = \frac{F_m - F_0}{F_m}$
Photochemical effective yield PS II	Φ_{PSII}	$\Phi_{PSII} = \frac{F_m^L - F_t}{F_m^L}$
Non-photochemical quenching	q_N	$q_N = 1 - \frac{F_m^L - F_0^L}{F_m - F_0}$
Photochemical quenching	q_P	$q_P = \frac{F_m^L - F_t}{F_m^L - F_0^L}$
Stern-Volmer coefficient of non-photochemical quenching	NPQ	$NPQ = \frac{F_m - F_m^L}{F_m^L}$

The instrument used for the analysis of fluorescence images is the Open FluorCam FC 800-O (Photon Systems Instruments), shown in the Figure 2.10. It is an instrument with flexible geometry enabling work with samples of various sizes. The Open FluorCam FC 800-O consists of a CCD camera (charge-coupled device) with a particular sensor for image capture, four fixed LED panels to which they can be applied 7 different emission filters. The four LED panels can be arranged at various angles and distance from the sample. The position of the camera may also be adjusted with respect to the sample height. One pair of LED panels provides Measuring Light ML and Actinic Light Act1 (red-orange 617 nm). Other two panels provide Actinic Light 2 Act2 and Saturating Pulse (cool white light, 6500 K). The instrument constructs the image in four phases:

1. capture of the image;
2. image segmentation;
3. analysis;
4. visualization.

The timing and amplitude of actinic irradiance are determined by user defined protocols. The instrument also includes a high-performance PC and comprehensive software package comprising full system control, data acquisition and image processing.The LED can in some cases be a source of error the measurement, despite the high performance (response interval below the second, light intensity twice as far as the sun), inasmuch the signal can hit the sample

in a non-homogeneous way. It is therefore necessary to make sure that the sample is correctly housed under the light source.

Once the signal has been sent to the sample under analysis, the CCD camera collects the fluorescence image after its passage in a filter that allows the passage of a light in red and in far red ($\lambda > 690$ nm). The dynamic images captured are digitalized via a digital convertor, in 12 or 14 bit data and transferred to the PC where they are stored. Finally, through the use of a specific software the data are processed to determine the photochemical parameters and generate images of fluorescence signal at any moment of the experiment and present them using a false color scale.

Depending on the sample to be analyzed and the data to be obtained a specific protocol must be set, that is the specifications concerning the shutter, Act1, Act2 and saturating pulse to be supplied to the program. The phase of choice of the measurements protocol plays a very important role since all the data obtained will depend on it, it must ensure that the data are consistent and that the noise of the instrument and of the sample do not interfere too strongly.

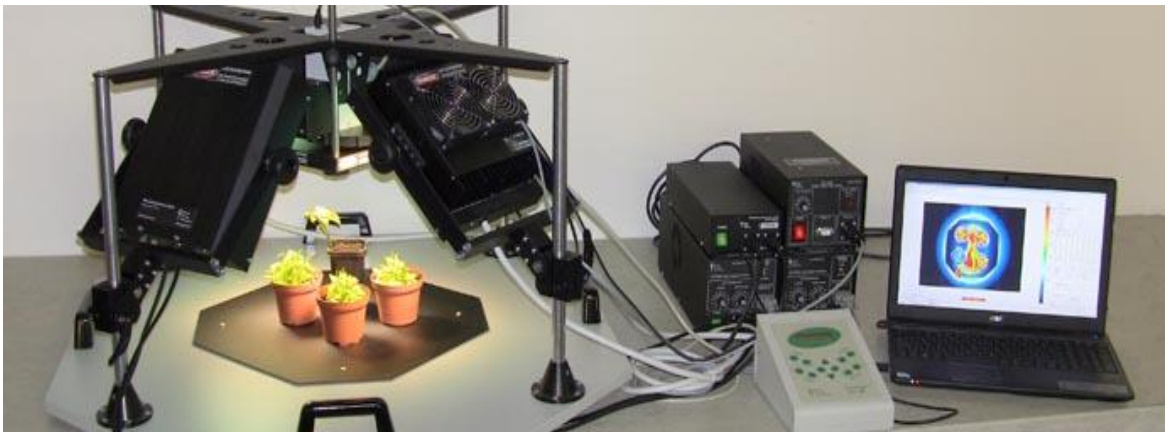

Figure 2.10 *Open FluorCam FC 800-O (System Instrumentation). (http://www.psi.cz/products/fluorcams/open-fc-800-o-1010)*

2.3.5 Fluorescence measurement protocol

Each measurement is preceded by a period of adaption in the dark, in this phase the sample is placed in a dark room. The adaption in the dark of a photosynthetic sample, has the purpose to obtain the complete oxidation of the plastochinone and therefore to open the reaction centers. This operation is necessary in order to measure the photosynthetic performance, in this specific case the background fluorescence (F_0) (Figure 2.8).

The need to carry out various measurements throughout the day has led us to evaluate the influence of the period of dark adaptation on the measure. Starting from a dark period of 20 minutes (Perin *et al*., 2016) we went down to 15 and finally to 5 minutes, the different measure of F_0 were compared and there was not a large variation between the measures conduced after

20 or 5 minutes. We therefore chose to adopt a dark adaptation period of 5 minutes, in this way the *in vivo* fluorescence measurement is closer to on-line measurement.
After a period of 5 minutes, a low intensity measurement light (ML) is activated which is not able to activate the photochemical process in which q_P=1 and q_N=0.
Under these conditions it is possible to measure F_0. In this work the values of F_0 were measured, as direct index of the chlorophyll content. Unlike F_m the background fluorescence values are less, because of this reason and of the background noise of the instrument (considered significant), the initial concentration of the inoculum (cells$\times 10^6$/ml) must be high enough to give a good response in F_0 (F_0 higher than the background noise of the instrument). Below are the values for the camera and light setting used in the analyses at the FluorCam software:

```
Shutter = 2;
Sensitivity = 5;
Act1 = 100;
Act2 = 20;
Super = 20;
```

The `Shutter` determines the duration of interval during which the electronic shutter is open (during the measurements). A `Shutter` equal to 2 means an aperture of 33 μs. The sensitivity of detection is defined by the `Sensitivity` = 5. The sensitivity scale is linear (0-100%), a low `Sensitivity` has been chosen to overcome the over-pixel problems of the instrument analysis.

2.4 Correlation of cell concentration - F_0

The correlation between cell concentration and fluorescence intensity was verified by inoculating the micro-PBR with 6 different concentrations each in quadruple copy (see Figure 2.11). Maintenance of the pre-cultured in the flasks is guaranteed by periodic refilling (every 3 or 5 days) of medium BG11, this allows to keep algae in the exponential phase.
The steps that precede the inoculum can be summarized as follows:

1. The pre-inoculum is taken from the flask (in the middle of the exponential phase) and the following analyses are performed: OD, DW and cell count with Bürker chamber, in order to assess the starting concentration.

2. Once the initial concentration of the pre-inoculum has been calculated, 2 or 4 eppendorf containing the pre-inoculum are then centrifuged (at 4 g for 2 min), the exhausted BG11

medium is removed and the microalgae are resuspended with a new pre-inoculum (this technique allows to quickly reach high cell concentrations), thus allowing explore a wide concentration range. The need to inoculate high cell concentrations is reported in section §2.3.4.

3. Obtained the desired cell concentration (120-150 cells$\times 10^6$/ml), proceed to serial dilution (with BG11) in order to obtain 12 different concentration (6 concentrations per microphotobioreactor in quadruple copy. Subsequentely the micro-PBR is inoculated by filling each well with 20 µl with a micropipette. Figure 2.11 shows 12 concentrations to be submitted to fluorescence measurement and the relative image obtained from the Open FluorCam FC 800-O.

4. The micro-PBR is closed with a layer in PDMS, sealed inside the closing unit, and placed under irradiation 50 µmol photons/(m^2 s).

5. After 30 minutes (time required by *Scenedesmus obliquus* to settle in the well), the micro-PBR is adapted to the dark for 5 minutes after which the fluorescence measurement is performed.

6. The fluorescence images are processed thanks to the FluorCam7 software (Photon System Instruments), obtaining F_0 for each well, easily visualized in a plot showing F_0 vs cells concentration (cells$\times 10^6$/ml) (Figure 2.12). Through the plot, it is possible to obtain the correlation that will allow to indirectly calculating the microalgae concentration during on the conduct of the experiments. The correlation is calculated through the knowledge of the inoculated concentrations and the corresponding measured F_0 values (Table 2.2). F_0 is expressed as average of 4 biological replicates. Data were fitted with a least square regression, obtaining a relationship in the form of $y = ax + b$.

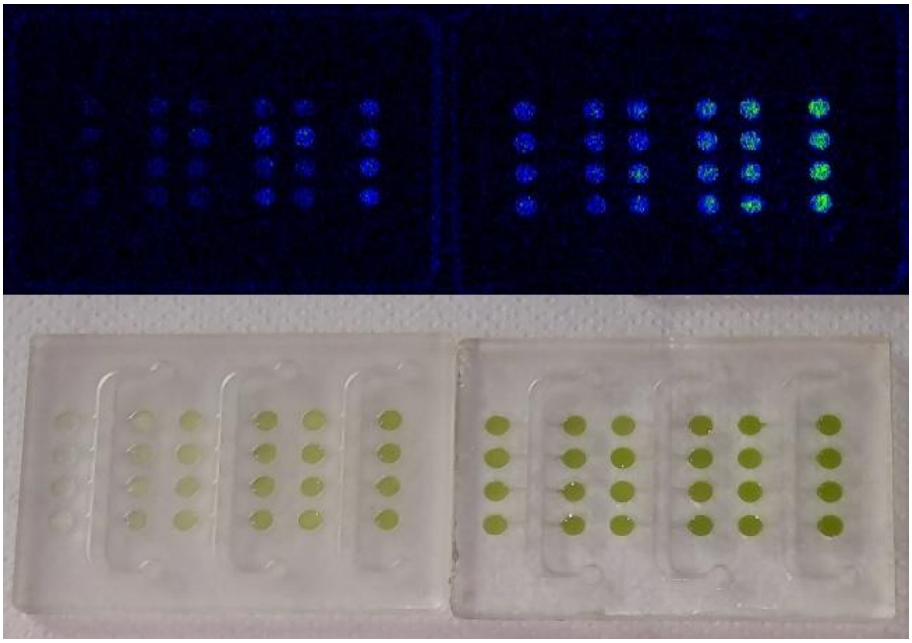

Figure 2.11 *Micro-PBR used to obtain the correlation between cell concentration and fluorescence intensity and relative images obtained from Open FluorCam FC 800-O.*

Table 2.2 *Cells concentration and F_0 values used to build up the growth monitoring method. The cell concentration values used to inoculate the micro-PBR are here reported (cell concentration). F_0 is expressed as average of 4 biological replicates. SD comes from data collected from wells inoculated in quadruple copy.*

Cell Concentration $\times 10^3$ cell/ml	F_0	SD_{F0}
103	191.3	9.69
89.3	167.3	7.52
77.4	145.4	4.45
67.1	118.0	7.42
58.1	98.5	6.12
50.4	96.4	3.25
43.7	94.1	2.38
31.5	71.1	1.81
27.3	65.6	3.48
20	57.6	7.10
13.3	56.5	3.79
7.1	44.0	2.22

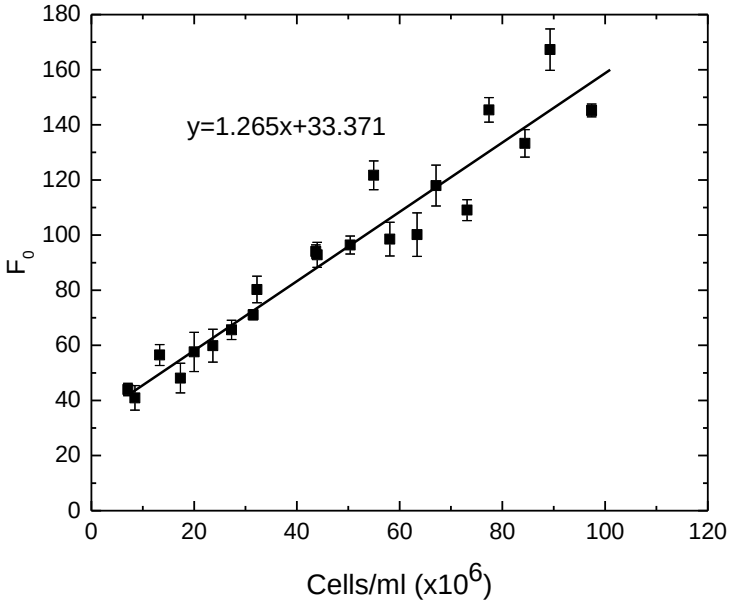

Figure 2.12 *The plot represents the correlation F_0 – cell concentration (cells×106/ml). Data are expressed as average of 4 biological replicates. The correlation are linear and data were fitting with a linear function (y = ax + b), represented by the solid line.*

The correlation was obtained through three different calibrations carried out with microalgae acclimatized to different conditions, for this reason this is a preliminary correlation (F_0 – cells concentration) for this reason, it must be investigated in the future. However, for the purpose of this work, it has been decided to use it for the estimation of the microalgae growth.

2.5 Cell growth protocol

The cell growth protocol remains unchanged with respect to the correlation of cell concentration and fluorescence intensity up to point 2, from which we proceed as follows:

1. Obtained the desired cell concentration (10-20 cells×10^6/ml), proceed to inoculation, each well is loaded with 20 µl. The micro-channels and the flow channels are now filled with BG11 medium at three different carbonate concentrations (see section §3.2.2).

2. The micro-PBR is closed with a layer in PDMS, sealed inside the closing unit (during this procedure it is essential to avoid the formation of air bubbles inside the chip), and placed under irradiation.

3. The three syringes as prepared as described in section §3.2.2 and are installed on the syringe pump: three syringes in infusion (50 ml) and two syringes in withdraw (50 ml).

The syringes that work in withdraw are partially filled with water (~10 ml) to facilitate the balancing of the pressure inside the micro-PBR.

4. The syringes are connected to the micro-PBR through the use of Tygon® tubes (diameter 1.5 mm), the positioning of the tubes is a delicate procedure to which great attention must be paid. Three tubes connect the syringes in infusion with the alimentation holes of the chip, two tubes connect the syringes in withdraw with the outlet holes and one tube will be connected to an outlet hole and will work by capillarity. This workaround is necessary since the available rack in the pump allows only the positioning of two withdraw syringes.

5. A pump flow of 8 µl/min is set, this allows not to disturb the microalgae inside the micro-PBR and to prolong the experiments for several days (3-4 days). 8 µl/min corresponds to ~11 ml per day, loading a total of 50 ml (per syringe), the experiment can be prolonged for several days.

6. The micro-PBR will be subject to 4 daily fluorescence analyses, the images obtained will be processed to obtain the microalgae growth profile (Figure 2.13).

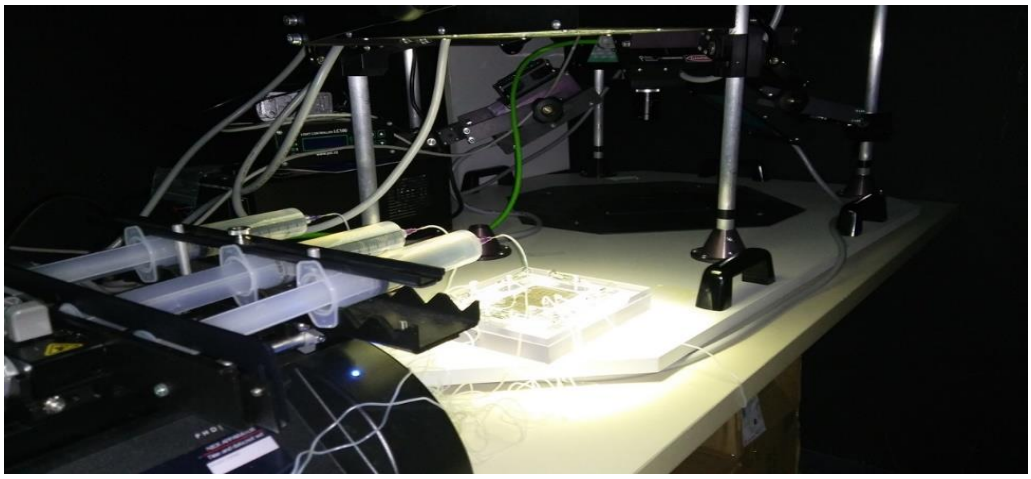

Figure 2.13 *Experimental set-up*

Chapter 3

Design of the culture system

In this chapter, we will explain in details all the technical and design progresses that allowed to develop, from an experimental point of view, a final version of an efficient CO_2 supply system for microalgae growth in microphotobioreactors (chip).

3.1 Analysis of CO_2 limitation in previous chip configuration

The initial phase of this work was characterized by a period of investigation. The purpose of this preliminary investigation was first to assess the contribution of carbon dioxide, through the nutrient flow, to the microalgae with a qualitative and quantitative approach. The experimental setup consists in a microphotobioreactor (Figure 3.1a) in PDMS closed by the overlap of a layer made of the same material (Baseotto, 2016) and a closing unit (Figure 3.1b). The main purpose of the closing unit is to keep the system sealed and prevent leaks, since the system is designed to work with a flow regime. In fact, this type of system was designed to guarantee a continuous feed of nutrients and a stable diffusion gradient thus ensuring a precise control of the nutrients concentration using two flows, one rich in the nutrients and other without them.

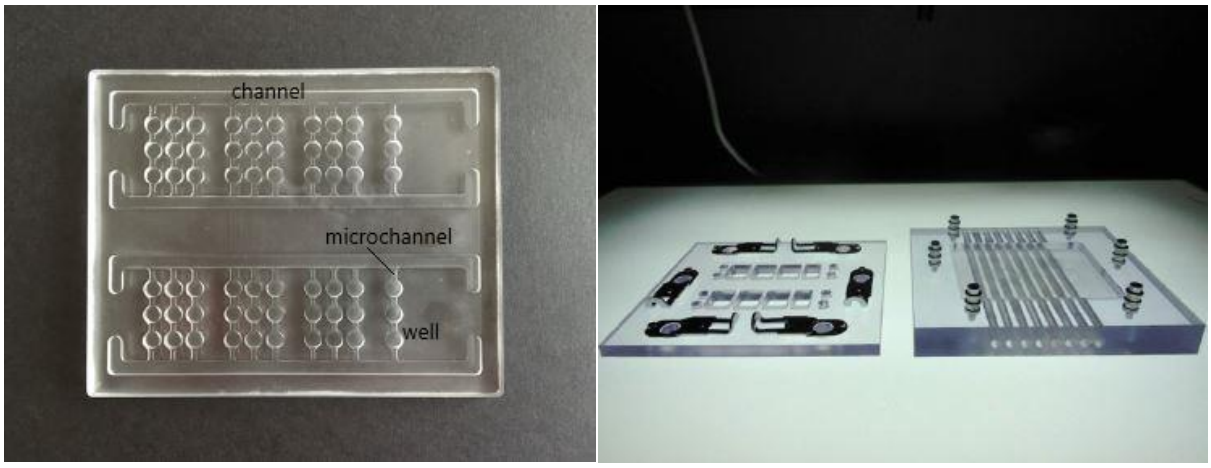

(a) (b)

Figure 3.1 *Microphotobioreactor and closing unit (Baseotto, 2016).*

The aim of this system was to establish a concentration gradient of the chemical species (NO_3^- and micronutrients) whose growth effect was to be evaluated. The dimensions of the microphotobioreactors were 96×75×5.25 mm (L×W×H), the wells had a diameter of D = 4 mm and depth H = 3.25 mm, while the microchannels had a square cross-section equal to 1x1 mm. 60 wells were present one chip with a volume of 40 µl each.
Experiments carried out with colorants gave unsatisfactory results since the main difficulty was to guarantee a homogeneous seal with consequent lack of formation of the diffusion gradient.
For this reason, the geometry of the micro-PBR was completely re-designed, avoiding the creation of diffusion gradients in the first place, but using instead different inlets where the nutrients concentrations can be specifically controlled.
In this work thesis, another issue has been tackled, regarding carbon dioxide concentration inside the well. As previously denoted, CO_2 is one of the main nutrient for photosynthesis and it directly impacts on the microalgae growth, it is therefore of primary importance to establish whether the operating conditions are limiting or not for the biomass growth. Taking as reference the first well in the geometry used in the work by Baseotto (sketched Figure 3.2), preliminary study on CO_2 limitation was conducted.

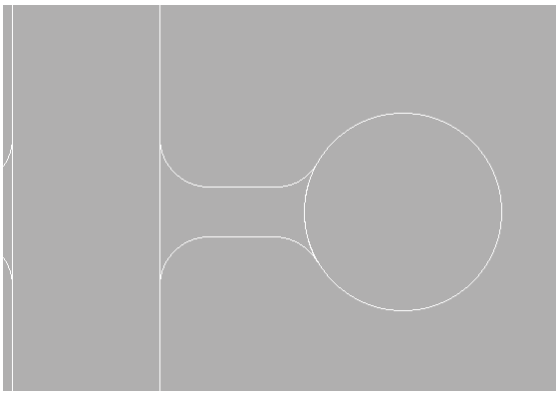

Figure 3.*2* *Schematic representation of microchannel and well. (Baseotto, 2016)*

The aim of this section is therefore to evaluate the CO_2 concentration that should be supplied in the main channel (feed channel) through the medium.
Two balances were applied, one concerning the microchannel that connects the well to the feed channel and one based on the well.

- Mass balance in the microchannel

$$Acc = In - Out + Gen \qquad V = constant \tag{3.1}$$

$$V\frac{dC_{CO2}}{dt} = \dot{N}_{CO2} - r_{CO2}V = \dot{n}_{CO2}\,A^{m.channel} - r_{CO2}V = \tag{3.2}$$

The Equation 3.1 represents a generic balance. Considering a cross-section of the microchannel we can write the Equation 3.2, the accumulation term (*Acc*) is considered as zero, since the

study has been sized in the limit condition, e.g. in the condition in which all carbon dioxide supplied is consumed by microalgae. The term related to the flow (*In* and *Out*) is described by diffusion (Fick's law) only since in the microfluidic devices, it is a dominant phenomenon respect to the convection. Then rewriting the last equation, the following one can be obtained:

$$-D_{CO2/water}\frac{dC_{CO2}}{dx}A^{microchannel} - r_{CO2}V \tag{3.3}$$

$$-D_{CO2/water}\frac{(C_{CO2,channel}-C_{CO2}^{well})}{l}A^{m.channel} - r_{CO2}V \qquad \left[{}^{mol}/_{s}\right] \tag{3.4}$$

In Equation 3.4 the generation/consumption term is set equal to the consumption rate of carbon dioxide (CO_2 required for microalgal growth in the well) multiplied by the volume. The $C_{CO2,\ channel}$ represents the concentration of CO_2 in the feeding channel and consequently in the microchannel. Balance related to the well are reported:

- Well balance

$$Acc = In - Out + Gen \qquad V = constant \tag{3.5}$$

$$V\frac{dc_X}{dt} = r_X V^{well} = R_X = \left[{}^{mol}/_{s}\right] \tag{3.6}$$

To describe Equation 3.6, it is necessary to introduce the Monod kinetics, one of the earliest and most often used equations for describing the relationship between substrate concentration, in this case the CO_2 and biomass growth rate. The auto-catalytic nature of cell growth leads to a sigmoid curve (Figure 1.4) in a batch bioreactor. Therefore, the growth kinetic of microalgae biomass is formulated as a function of cell and substrates concentrations:

$$r_X = \frac{\mu \cdot C_s \cdot C_X}{K_M + C_s} = \left[\frac{mol}{d \cdot L}\right] \tag{3.7}$$

where μ is the maximum growth rate for the considered specie and C_s and C_X are the concentration of substrate (C_{CO2}^{well}) and biomass, respectively. The maximum growth rate and the saturation constant K_M are two constants parameters.

If the concentration of substrate in the bioreactor or microphotobioreactor *Cs* is much greater than the saturation constant, then the biomass specific growth rate equals the maximum specific growth rate and therefore the substrate is not rate limiting. On the other hand, if the substrate concentration is less than the saturation constant, then the specific growth rate drops below the maximum and the substrate becomes rate limiting. Therefore, the constant K_M is defined as the concentration of substrate at which the growth rate is half of the maximum value and it accounts for the decrease of the growth rate due to the lack of substrate. For the solution of two balances, the rate of consumption of the carbon dioxide (r_{CO2}) is set equal to the production rate of

biomass (r_X), divided by a yield coefficient ($Y_{X/CO2}$). The volumes are equal placed and the rate of consumption in Equation 3.8 is negative with respect to the production rate.
We assume that the CO_2 supplied is sufficient and not limiting for the microalgae growth.

$$r_{CO2}\,V = -\frac{1}{Y_{X/CO2}}\,r_X\,V^{well} \qquad V = V^{well} \tag{3.8}$$

We can now write:

$$r_{CO2}\,V^{well} = -\frac{1}{Y_{\frac{X/CO2}{CO2}}}\,\frac{\mu_{max\,growth} C_X C_{CO2}^{well}}{K_M + C_{CO2}^{well}}\;V^{well} \tag{3.9}$$

Which, of the substitution in Equation 3.4, leads to:

$$0 = -D_{CO2/water}\,\frac{(C_{CO2,channel} - C_{CO2}^{well})}{l}\,A^{m.channel} - r_{CO2}V^{well} \tag{3.10}$$

We obtain:

$$\frac{1}{Y_{X/CO2}}\,\frac{\mu_{max\,growth} C_X C_{CO2}^{well}}{K_M + C_{CO2}^{well}}\,V^{well} = D_{CO2/water}\,\frac{(C_{CO2,channel} - C_{CO2}^{well})}{l}\,A^{m.channel} \tag{3.11}$$

Where $Y_{X/CO2}$ represents the yield of CO_2 in biomass, in Equation 3.11 there are three unknowns variables: C_X, C_{CO2}^{well} and $C_{CO2}^{channel}$. To simplify the balance resolution, it was necessary to look for values that could concretely represent the concentrations within the microphotobioreactor. It was of primary importance to understand which range of biomass concentrations (C_X) adopt, since the fluorescence phenomenon is directly related to the amount

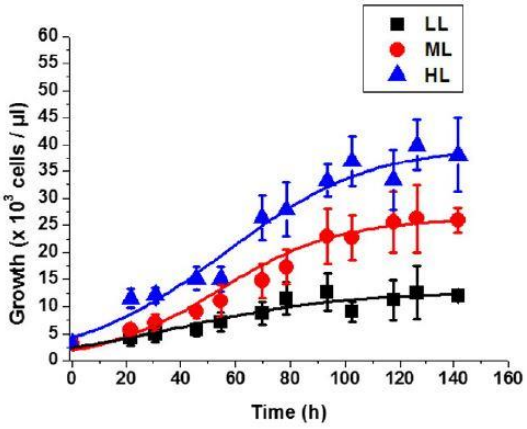

Figura 3.3 *Growth curves of Nannochloropsis gaditana cells at three chosen light intensities. LL (low light – 6 µmol photons/(m²s)), ML (medium light - 60 µmol photons/(m²s)) and HL (high light - 360 µmol photons/(m²s)). (Perin et al., 2016)*

of microalgae, through the correlation calculated in Chapter 2. Considering a previous work and looking at Figure 3.3, although it is based on a different microalgae specie, we can roughly estimate the maximum concentration achieved during a typical growth curve experiment, which is inside the linearity range (Perin *et al*., 2016).
The cell concentration assumed is 30× 10^3 cell/µl (blue line-high light). By assuming a weight per cell equal to 12 pg cells^{-1} (Lavens and Sorgeloos, 1996), a list of the parameters and values risulted:

- $C_X = 360\ g/m^3$
- $K_M = 4.75\ g/m^3$ (Concas *et al*., 2012)
- $\mu_{max\ growth} = 0.7\ \frac{1}{d} = 8.1 \cdot 10^{-6}\ \frac{1}{s}$ (McCormick *et al*., 1996)
- $Y_{X/CO2} = \frac{1}{1.83}\frac{kg_X}{kg_{CO2}} = 0.56\frac{kg_X}{kg_{CO2}}$

By setting now the values of concentration of CO_2 (C_{CO2}^{well}) in the well, it has been possible to solve the Equation 3.12 and the results is shown in Figure 3.4, which describes the growth rate as a function of the CO_2 concentration in the well.

$$r_{CO2} = -\frac{1}{Y_{X/CO2}}\frac{\mu_{max\ growth} C_X C_{CO2}^{well}}{K_M + C_{CO2}^{well}} \qquad (3.12)$$

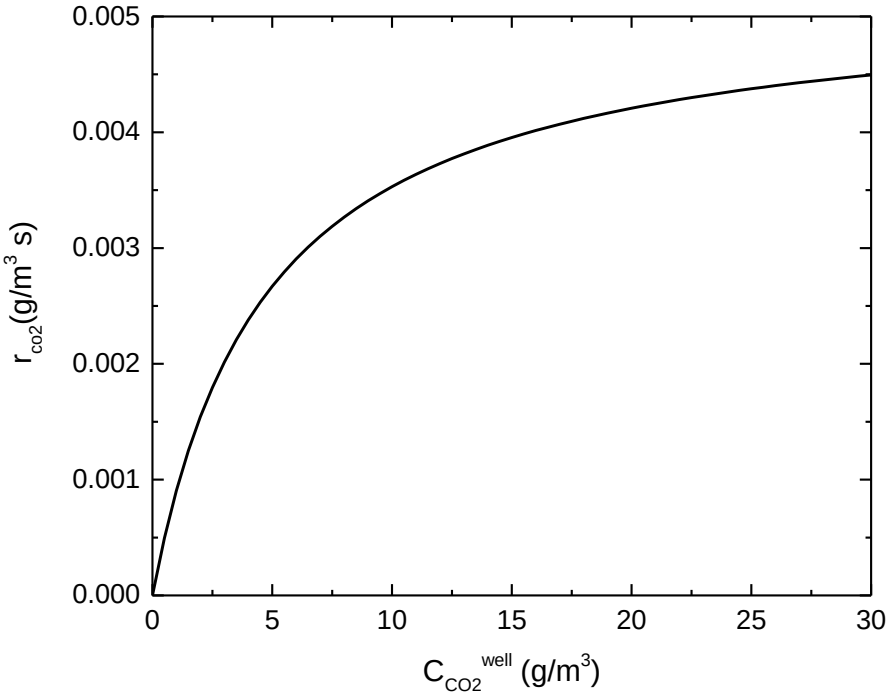

Figure 3.4 *Evolution of microalgae growth rate as a function of CO_2 concentration in the well.*

The increase in r_{CO2} is negligible once CO_2 concentration in the well reaches 20 g/m^3, thus deducing that in this condition carbon dioxide concentration is not limiting microalgae growth (Figure 3.4).
It was possible to calculate, through the Equation 3.13, the CO_2 concentration required in the channel to meet the demand for carbon dioxide in the wall.

$$C_{CO2,channel} = \frac{1}{Y_{\frac{X/co2}{CO2}}} \frac{\mu_{max\ growth} C_X C_{CO2}^{well}}{K_M + C_{CO2}^{well}} V^{well} \frac{l}{A^{m.channel} D_{CO2/water}} + C_{CO2}^{well} =$$

$$= 282.996 \frac{g}{m^3} \cong 0.3 \frac{g}{l} \quad (3.13)$$

- $A^{m.channel} = 1 \times 10^{-6} m^2$
- $V^{well} = 40 \mu l = 4 \times 10^{-8} m^3$
- $D_{CO2/water} = 1.92 \times 10^{-5} \frac{cm^2}{s} = 1.92 \cdot 10^{-9} \frac{m^2}{s}$ (Cussler, 1997)
- $l \cong 0.003\ m$ channel length

Knowing the concentration of carbon dioxide inside the channel (required for the microalgae growth) it is now necessary to calculate how much carbon dioxide is normally dissolved in a liquid under standard condition (ambient temperature and pressure).
The volume percent of CO_2 in dry air is 0.032%, leading to a partial pressure of 3×10^{-4} ($10^{-3.5}$) atm. Carbon dioxide is slightly soluble in pure water, as with all gases, the solubility decrease with temperature. At pressure up to about 5 atm, the solubility follows Henry's law (Lower, 1999):

$$[CO_2]=K_H \cdot P_{CO2}=0.032 P_{CO2} \quad (3.14)$$

Once it is has dissolved, a small portion of the CO_2 reacts with water to form carbonic acid:

$$[CO_2(aq)]=650[H_2CO_3] \quad (3.15)$$

Thus, what we usually refer to as "dissolved CO_2" consists mostly of the hydrated oxide CO_2(aq) together with a small amount of carbonic acid (a period of a few tenths of second is typically required for this equilibrium to be established). Water exposed to the atmosphere with $P_{CO2} = 10^{-3.5}$ atm will take up carbon dioxide until, from Equation 3.14:

$$[H_2CO_3]=10^{-1.5} \times 10^{-3.5}=10^{-5}\ M \quad (3.16)$$

with a molecular weight of 44 g/mol we obtain a CO_2 concentration equal to 4.4×10^{-4} g/l. This concentration is far lower than that required in the channel to operate in non-limiting CO_2 conditions (Equation 3.13). It was therefore necessary to evaluate a method for storing more CO_2 inside the BG11 medium.

3.2 Setup of a CO_2 absorption protocol

The following paragraphs discuss the CO_2 absorption by solutions composed of water and salts at different molarity. The CO_2 absorption capacity varies with the CO_2 partial pressure and with the salts concentration, to quantify in a rigorous manner the CO_2 amount in the liquid a software able to study the equilibria was used.

In order to quantitatively establish the CO_2 concentration in the culture medium, a sensitivity analysis was necessary. The simulations have been carried out with the use of Aspen Plus ® process simulator. At the beginning, process scheme has been created (Figure 3.5), the process of liquid saturation with CO_2 has been idealized as a tank with two separate inlet streams. The tank stands for the bottles where the medium is uploaded to allow the saturation with CO_2, and the two inlets represent respectively, one the air/CO_2 flow and the other one the medium flow. During the simulations, the medium has been represented as water with different concentrations of different salts.

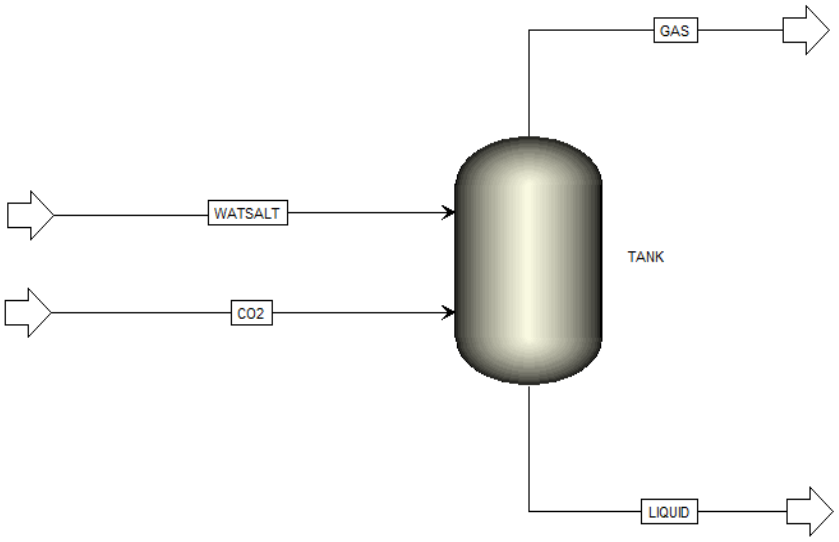

Figure 3.5 *Process representation.*

At first, the liquid behaviour has been studied by varying the ratio air/CO_2 in the inlet flow, examining the results (Figure 3.6) it has been decided to opt for a 100% CO_2 flow, this choice allows to obtain a higher concentration of CO_2 in the liquid and require only one CO_2 tank and only one pressure reducer.

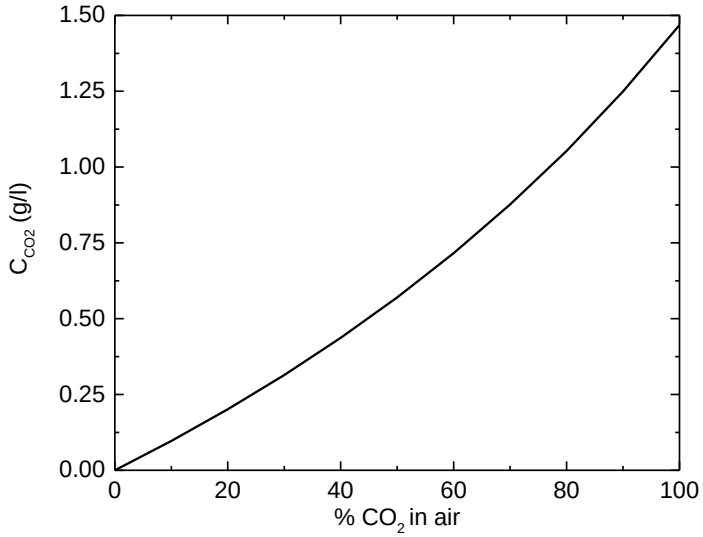

Figure 3.6 The plot describes the variation of the CO_2 concentration in fresh water when the CO_2 partial pressure changes.

The equilibrium of CO_2 in water is expressed as follow:

$$CO_2(g)+H_2O \leftrightarrow H_2CO_3(aq) \quad (3.17)$$

$$H_2CO_3(aq) \leftrightarrow HCO_3^-(aq)+H^+(aq) \quad (3.18)$$

$$HCO_3^-(aq) \leftrightarrow CO_3^{2-}(aq)+H^+(aq) \quad (3.19)$$

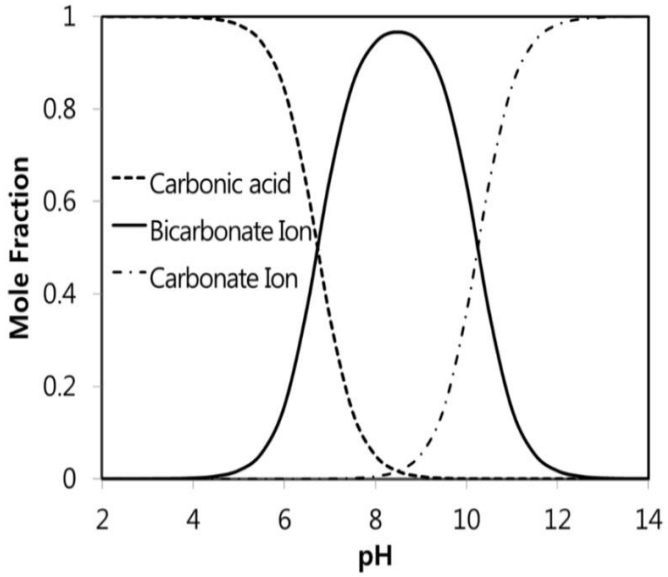

Figura 3.7 *Bjerrum plot, pH vs. the mole fraction of carbonate species (Shim et al., 2016).*

Carbon dioxide is a typical acid gas. First, gaseous CO_2 is dissolved in water (Figure 3.7), and it forms carbonic acid (H_2CO_3). The carbonic acid donates a proton (hydrogen ion, H^+) and forms a bicarbonate ion (HCO_3^-). The bicarbonate ion donates a proton and generates a carbonate ion (CO_3^{2-}). If we introduce the pseudo-steady state condition, (in this condition, $C_{total}=[H_2CO_3]+[HCO_3^-]+[CO_3^{2-}]$=constant), the mole fraction of each carbonate species could be expressed as a function of pH. The mole fraction of carbonate species is plotted in Figure 3.7, which is called Bjerrum plot (Shim *et al.,* 2016).

Therefore, observing the Equation 3.19 it follows that, with the increase of the CO_2 dissolved in water, the carbonic acid increases with a consequent decrease in the pH. For overcome this problem the solution was buffered with the use of carbonate and bicarbonate, compatibles with microalgae growth and able to normalize the pH.

Different types of salt have been tested at different concentrations in the water inlet flow. It has been hypothesized to have a water inlet flow equal to 100 kg/hr and a CO_2 flow equal to 50 kg/hr, this quantity proved to be sufficient for the liquid saturation. First, the effect of sodium bicarbonate has been tested, changing the molarity until 0.4M and keeping the CO_2 flow constant, and later the sodium carbonate has been tested in the same way. Taking into account the use in future experimentation of microalgae that require a saline medium, the tests have been carried out also for seawater this has been simulated by adding 30 g/L of NaCl. The operating conditions at which the tests have been carried out, respect the standard conditions, that are 1 atm and 25°C and also the conditions under which the experiments have been performed.

Below will be briefly described the steps followed during the simulations in Aspen Plus®.

The Properties Specifications Global sheet is used to enter the thermodynamic methods used to calculate the properties used in the simulation. The Electrolyte-NRTL activity coefficient model (ELECNRTL), is the recommended option set for simulations with electrolytes. ELECNRTL, calculates liquid phase properties from the Electrolyte-NRTL activity coefficient model. It is advisable to use the Electrolytes Wizard, to define the ionic species and salts that can be generated from the base components entered on the Components Specifications Selection sheet, and to generate the reactions that occur among these components in the liquid phase.

An electrolyte system is defined as one in which some of the molecular species dissociate partially or completely into ions in a liquid solvent, and/or some of the molecular species precipitate as salts. These dissociation and precipitation reactions occur fast enough that the reactions can be considered to be at chemical equilibrium. The liquid phase equilibrium reactions that describe this behaviour are referred to as the solution chemistry. In Aspen Plus®, solution chemistry is often referred to simply as chemistry. Solution chemistry has a major impact on the simulation of electrolyte systems. In Aspen Plus®, all unit operation models can

handle electrolyte reactions. Solution chemistry also impacts physical property calculations and phase equilibrium calculations.

When using the true component approach, Aspen Plus® solves the equations describing solution chemistry simultaneously with the unit operation equations. The unit operations deal directly with the ions and salts sheeted by solution chemistry. In addition, the true component approach defines how the process simulator reports the simulation results. Results are reported in terms of the ions, salts, and molecular components that are actually present, not in terms of the original base components.

3.2.1 Results of simulation

After the different simulations, the data have been collected in an Excel file for the analysis. The results have been based on both molar and massive flows in outlet of the tank and plots have been drawn. The first two plots represent the simulations performed with $NaHCO_3$.

In the first case, the plot represents the solution with fresh water while in the second case with seawater.

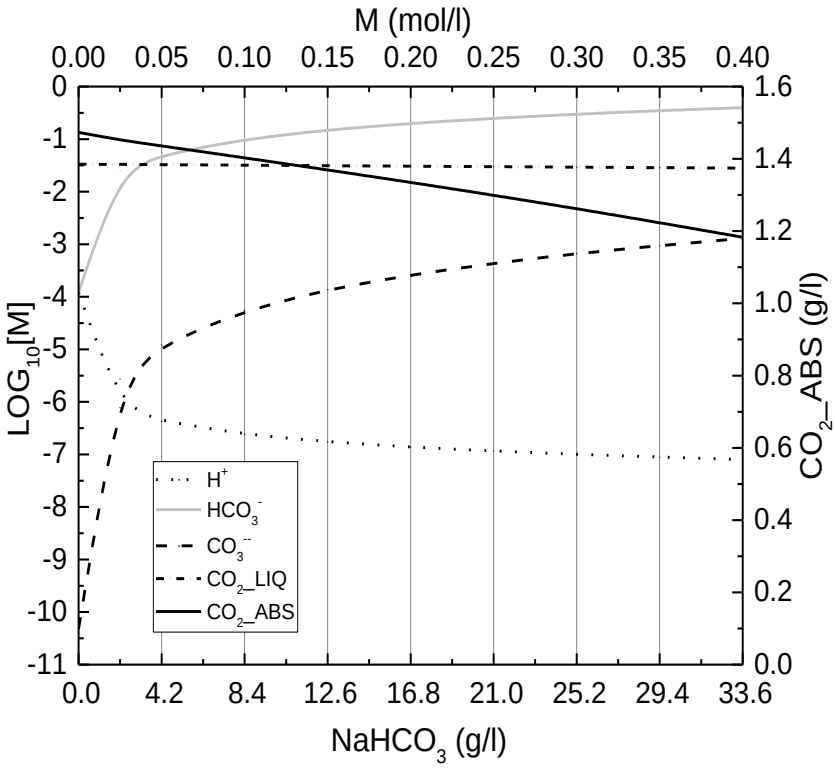

Figure 3.8 *Fresh water with $NaHCO_3$ at different molarity with a 100% CO_2*

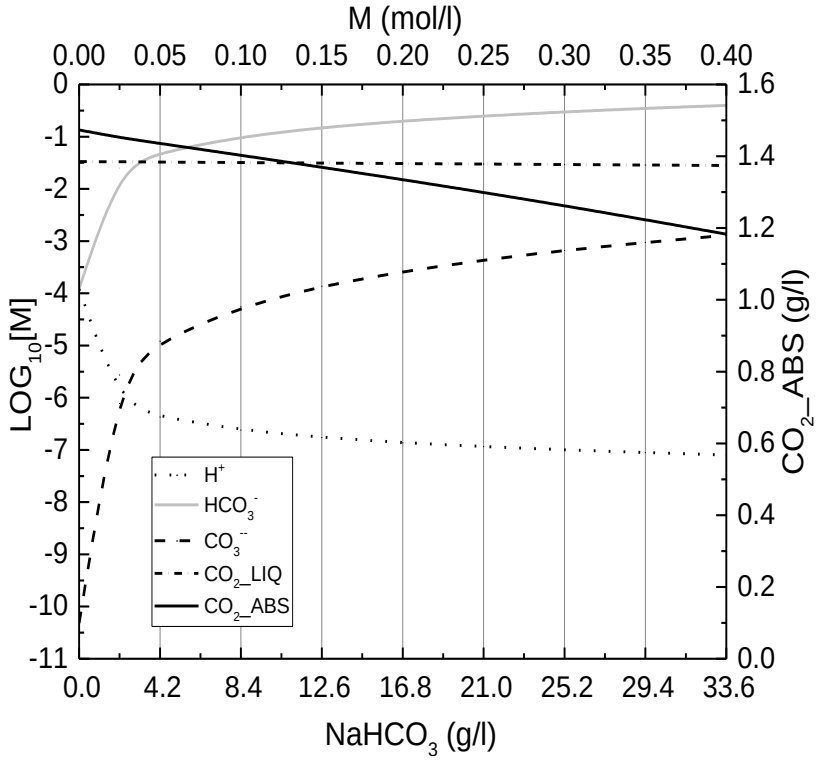

Figure 3.9 *Seawater with $NaHCO_3$ at different molarity with a 100% CO_2 flow*

The plots that follow represent the simulation with Na_2CO_3 and as before in the first case the plot represent the solution with fresh water while in the second case with seawater.

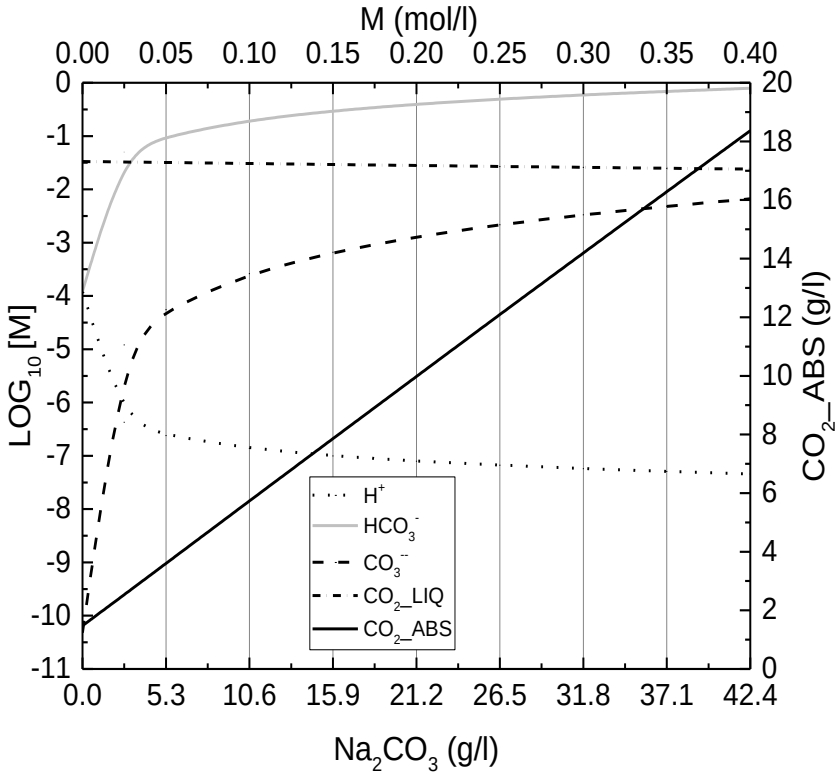

Figure 3.10 *Fresh water with Na_2CO_3 at different molarity with a 100% CO_2 flow.*

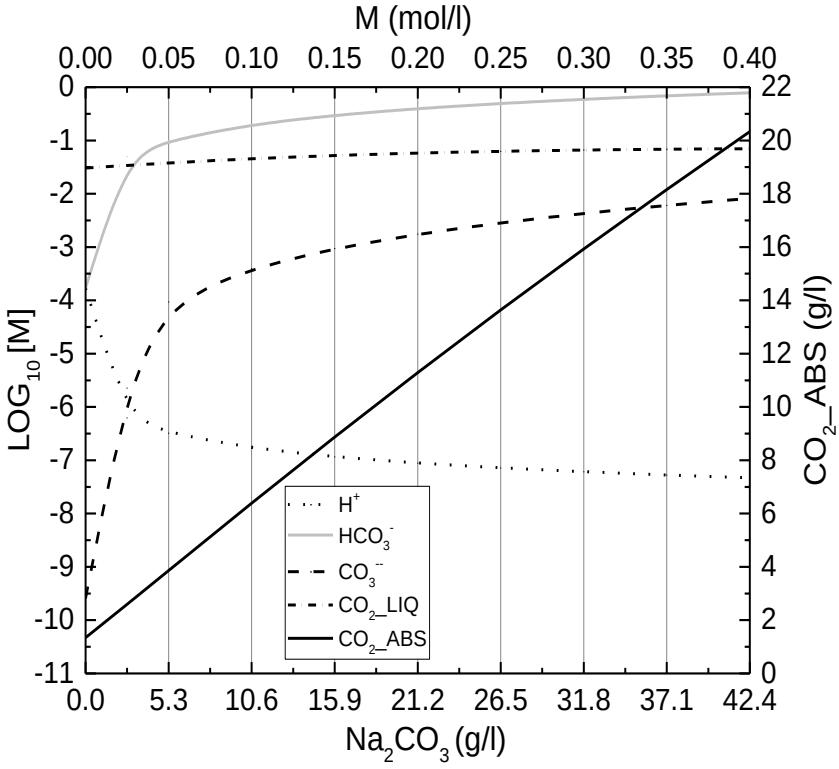

Figure 3.11 *Seawater with Na_2CO_3 at different molarity with a 100% CO_2 flow*

The plots reported in a y-axis the ionic concentration as a logarithmic scale (H^+, HCO_3^-, CO_3^{--}, $CO_{2\text{-}LIQ}$) and in the y-axis on the right section the CO_2 absorbed in terms of concentration (g/l). The CO_2 liquid concentration in logarithmic scale has a constant trend regardless the molarity but its value changes according to the kind of salt and the type of water. It can be noted how the use of sodium carbonate allows to have a greater concentration of C in the liquid, with pH values compatible with the microalgae optimal growth conditions. In fact, it is shown that alkaline aqueous solutions resulting from the dissolution of salt such Na_2CO_3, provides an excellent gas-liquid interface for CO_2 capture, leading to significantly enhanced CO_2 sorption capacity and kinetics (Cai *et al.*, 2018).
By adding this type of carbonates to the BG11 medium the equilibria is shifted and the overall results is an increase amount of carbon in the medium.

3.2.2 Experimental validation

The validation in the laboratory consists in the preparation of different solutions at different molarity of sodium carbonate and water. The different solutions are then loaded with a bubbling of CO_2 (100% CO_2 flow). Through the use of a pH meter and plots shown in the section §3.2.1, it was possible to validate the data obtained through the simulations in Aspen Plus.
Operating conditions:

- T = 298.15 K

- P = 1 atm

The salt is first dehumidified and then added to the deionized water (100 ml). Obtained a homogeneous solution, a flow of CO_2 is bubbled and at constant intervals of time the pH is measured until equilibrium is reached. The data relating to laboratory experimental validation are show in the Table 3.1.

Table 3.1 *The table shows the molarity values and the relative grams per litre of Na_2CO_3. In the third and fourth columns the initial and final measured pH values of the solutions are reported, the fifth column shows the pH data obtained through the simulation in Aspen Plus ®, the last column represents the relative error ($\varepsilon_{relative}$=(Final pH - Expected pH)/ Expected pH × 100).*

M (mol/l)	Na_2CO_3 (g)	Initial pH	Final pH	Expected pH	Time (h)	$\varepsilon_{relative}$
0.05	0.5	11.11	6.71	6.62	1	1.36%
0.15	1.6	11.16	7.13	7.00	1.5	1.85%
~0.25	2.6	11.20	7.29	7.00	2.5	1.53%
~0.35	3.7	11.28	7.41	7.29	2.5	1.65%

It can be noted how, as the concentration of Na_2CO_3 increased, the time achieving equilibrium increased. It is therefore recommended to use stirring bars inside the loading bottle to allow a more affective break of CO_2 bubbles and thus maximize the mass transfer. The plots obtained through the simulations have been validated from an experimental point of view and then used as a measuring instrument in the preparation of the culture medium.

For the experiments, three different medium have been prepared at three different Na_2CO_3 concentrations:

- BG11

Figure 3.12 *CO_2 loading system.*

- BG11 2.5 g/l Na_2CO_3
- BG11 10 g/l Na_2CO_3

The medium have been loaded with CO_2 (Figure 3.12), checking the initial pH and the final pH (procedure described in section §2.5 point 3).

3.3 Final micro-PBR prototype

Finally, it has been necessary designed a new micro-PBR (Figure 3.13) that allowed to investigate the efficiency of a medium with higher CO_2 concentrations on microalgae growth. The final prototype has been designed that would respect the following specifications:

- Develop a non-limiting nutrient flow (CO_2) inside the micro-PBR.
- Each well has been made independent of the others, in this way the influence of the other wells is avoided.
- Three independent alimentation channels that allow to carrying out three independent experiments, each channel feeds eight wells (three experiment with eight replicates each).
- Reduce micro-PBR size, to improve pressure control (to avoid preferential pathways).
- The feed channel has been widened at the entrance to allow the stabilization of the nutrient flow.
- The alimentation well and the outlet well have been made larger so as to favour the positioning of the Tygon® tubes (diameter 1.5 mm).
- Since the CO_2 will be provided directly through the medium and not from the atmosphere, the closed unit has been redesigned with fully-closed upper part.

Table 3.2 *Dimensions comparison between "Baseotto" prototype and final prototype.*

	Previous prototype	Final prototype
W (mm)	75	50
L(mm)	96	71.55

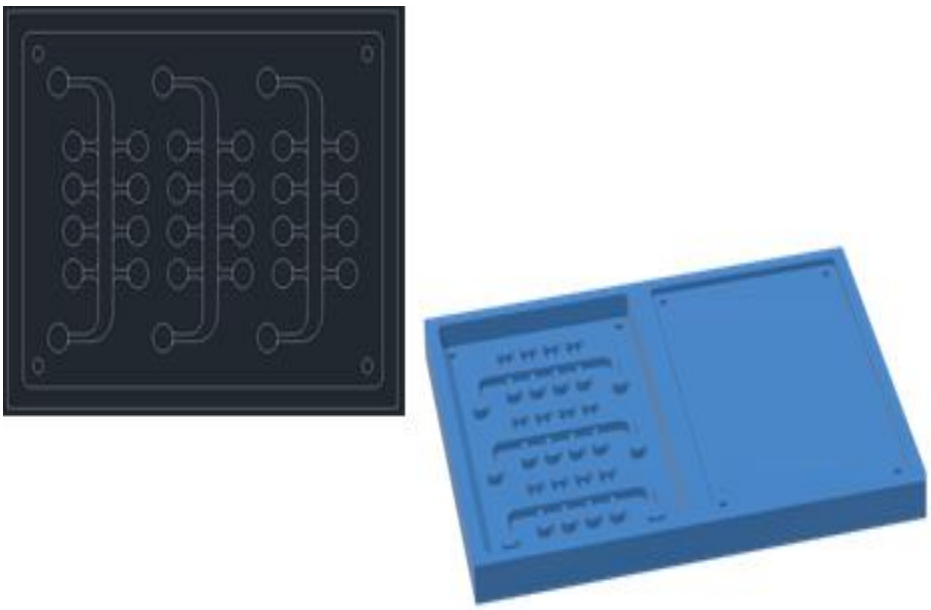

Figure 3.13 *Final prototype* ***(****Castaldello, 2018).*

On the new chip layout several fluid dynamic simulation have been performed. Practically a Tygon micro bore tubing represents the inlet (and the outlet). The simulation involved the behaviour is steady state of water flowing inside a chip made by polysilicon. The results, in terms of velocity inside the microfluidic device, are encouraging. In fact, the velocity is uniform (Figure 3.14), in the full range of velocity considered (5 µl/min). The difference between the inlet and the outlet in the figure is due to the walls effect: while in the inlet the specification on the velocity is a normal velocity, in the outlet the flow assumes a pattern typical of a flow inside a pipe.

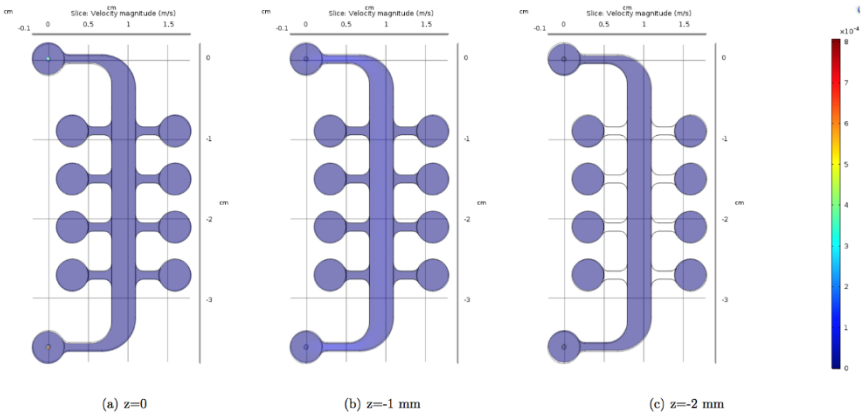

Figura 3.14 *Representation of the velocity field in the microfluidic device at steady-state, at different depths (z coordinates). (Castaldello, 2018)*

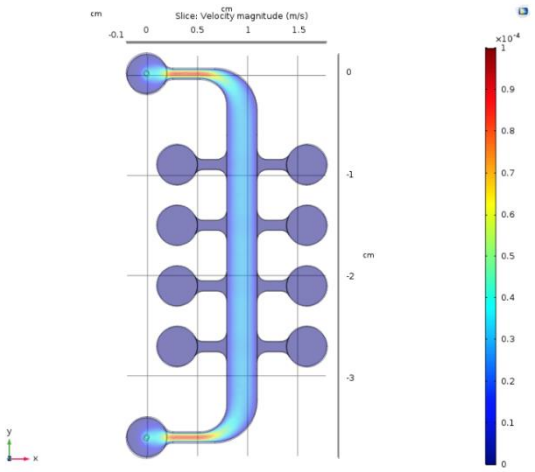

(a)

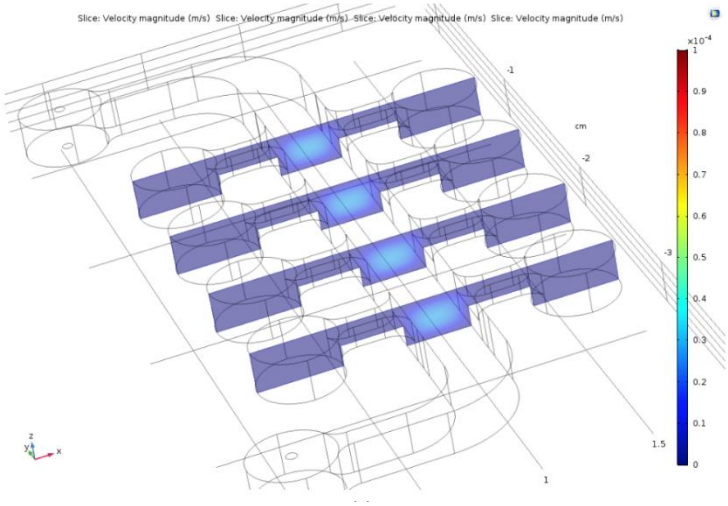

(b)

Figure 3.15 *Representation of the velocity with a reduced range, in different panels of the device: one panel to the fluid flow, and four perpendicular to it and placed at each microwell entrance. (Castaldello, 2018)*

In Figure 3.15(a) the range of velocity has been reduced, in order to enhance the fluid behaviour after the inlet. In Figure 3.15(b), the velocity at each microwell entrance is shown, and it appears clear that each microwell is affected by the same channel condition. (Castaldello, 2018) The development of this new prototype allowed to carry out three different experiments at the same time, with eight biological replicates for each one.

Chapter 4

Experimental results and discussion

In this chapter, results obtained from the experimental tests will be reported. In order to assess the influence of carbon dioxide on the microalgae growth objectively, two experiments have been performed, with and without the addition of CO_2 bubbling in the culture medium (BG11). Based on the results obtained, different plots have been reported with the aim of comparing the different conditions of growth. Finally, the influence of light intensity on the best growth conditions found in the previous experiments has been evaluated.

4.1 Experiment results BG11 with Na_2CO_3

The objective of the first experiment concerned the evaluation of microalgae growth conditions in the presence of three different mediums. With the aim of uniquely characterizing the CO_2 effect on the next experiments, the culture medium of this test has been prepared with sodium carbonate. The medium have been prepared at three different concentrations: standard BG11, BG11 with 2.5 g/l and with 10 g/l of Na_2CO_3. Growth has been studied by inoculating the micro-PBR with a single starting cellular concentration (see section §2.5), cells pre-cultured in flaks at 50 μmol photons / (m^2 s) have been chosen. The design of final prototype allowed to obtain three different sections fed by different culture medium; every single section includes eight biological replicates for the same condition (Figure 4.1).

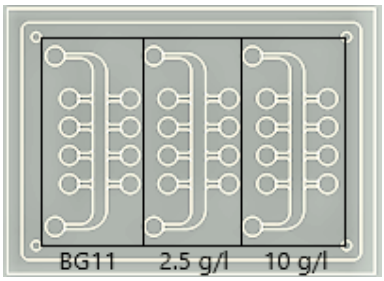

Figure 4.1 *Schematic representation of the three different sections fed by three different culture medium, BG11, BG11 with 2.5 g/l Na_2CO_3 and BG11 with 10 g/l Na_2CO_3.*

The chip has been exposed to an incident light intensity of 50 μmol photons / (m^2 s) and growth has been monitored four times a day by measuring the fluorescence intensity F_0 to estimate the

Chl content. The F_0 measures obtained for each region are the average of eight biological replicates.

The results obtained from this experiment, as previously mentioned, provided information about the ability of microalgae to grow in the presence of different sodium carbonate concentrations. The results obtained are shown in the plots of Figure 4.2, which represent the fluorescence intensity over time (a), the cells concentration over time (b), and the natural logarithm of the latter (c).

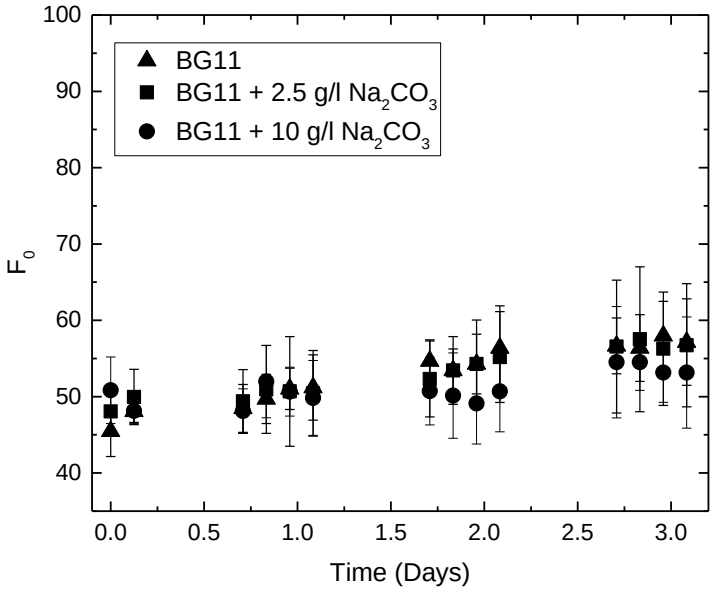

Figure 4.2*(a) Comparison of growth curves of Scenedesmus obliquus obtained using different concentration of sodium carbonate (0, 2.5, 10 g/l, represented respectively as triangles, squares, and circles). Plot showing the chlorophyll F_0 values as a function of time.*

The Chl fluorescence depends on the Chl microalgae content in the wells and therefore can be used as an indirect measure of cellular concentration. In order to obtain a quantitative description, a preliminary correlation of cell concentration and fluorescence intensity has been found (see section §2.4).

This correlation represent a rough tentative to quantify microalgae and it must be further verified and validated to ascertain possible variation of fluorescence in cells adapted to different light intensities. However, this is beyond the scope of this thesis work. In this case, it was used to preliminary estimate concentration in such microsystem. The correlation between fluorescence intensity and cells concentrations allowed to calculate the specific growth rate, and to compare different growth conditions. Through the fitting, the specific growth rates have been calculated as a logarithmic fit of the exponential growth phase (in this phase the growth rate is proportional to the number of cells present). The data obtained are sufficient for a

comparison between the various experiments carried out in this thesis work, but particular attention will have to be paid in comparing them with other data obtained from other cell concentration-fluorescence intensity correlation. The plot reported in Figure 4.2(a) represents the variation of the fluorescence intensity over time.

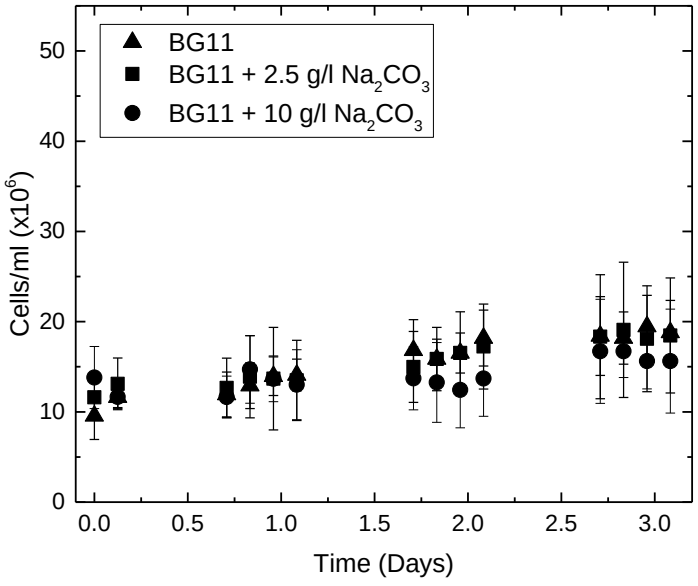

(b)

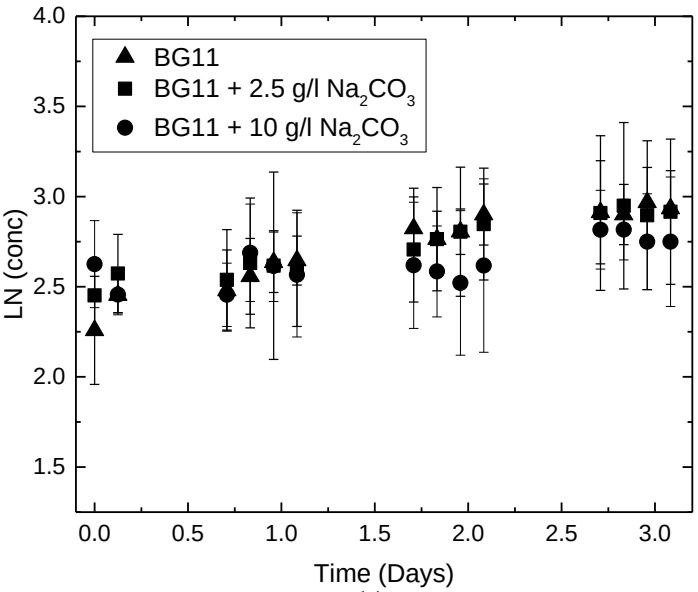

(c)

Figure 4.2 *Comparison of growth curves of Scenedesmus obliquus obtained using different concentration of sodium carbonate (0, 2.5, 10 g/l, represented respectively as triangles, squares, and circles). (b) The plot showing the cellular concentration (cell/ml (× 10^6)) as a function of time and (c) the plot showing the logarithmic fit of cellular concentration (cell/ml (× 10^6)) as a function of time.*

In Figure 4.2(b) the cell concentration (cell/ml (× 10^6) over time provided is reported through the correlation. Finally, in Figure 4.2(c) different specific growth rates have been comparted.

Based on results plotted in Figure 4.2, it is possible to affirm that with such carbonate concentration, the pH rapidly increase and the algal growth was strongly inhibited, with a very low specific growth rate.
In fact, the culture medium BG11, containing sodium carbonate presents a high pH value (Table 4.1), outside the optimum pH range of viability of algae cells. In addition, pH tends to increase during algae growth as a result of photosynthetic metabolism.

Table 4.1 *Represents the pH value of three different culture medium with three different sodium carbonate concentrations. The addition of carbonate caused a rapid increase of pH up to values close to 10-11.*

Na_2CO_3 (g/l) in the culture medium	pH
0	7.76
2.5	9.98
10	10.93

The inhibition of growth by sodium carbonate might also be explained by a specific inhibition due to the sodium ion (Gris *et al.*, 2014). In fact, it is demonstrated that osmotic effect and ionic effects are both involved in the induced inactivation of the photosynthetic machinery in the microalgae (Allakhverdiev *et al.*, 2000).
At lower concentration and at higher concentration of sodium carbonate (2.5 g/l of Na_2CO_3, 10 g/l of Na_2CO_3), specific growth rates of 0.150 d^{-1} and 0.05 d^{-1} have been measured, thus suggesting that *Scenedesmus obliquus* is not able to efficiently exploit carbonate as the carbon source as already reported in the literature (Gris *et al.*, 2014). The best response in this experiment has been given by the microalgae fed by BG11 without carbonate, with a specific growth rate of 0.23 d^{-1}.

4.2 Experiment results BG11 with Na_2CO_3 and CO_2

The objective of the second experiment concerns the evaluation of microalgae growth conditions in the presence of three different culture medium at three different molarity of sodium carbonate, loaded with a bubbling of CO_2 (100% CO_2 flow).
As for the previous experiment the micro-PBR has been divided into three sections, the first has been fed with BG11 + CO_2, the second with BG11 + 2.5 g/l of Na_2CO_3 + CO_2 and the third with BG11 + 10 g/l of Na_2CO_3 + CO_2.
Growth has been studied by inoculating the micro-PBR with a single starting cellular concentration, cells pre-cultured in flaks at 50 μmol photons / (m^2 s) have been chosen. The

chip has been exposed to a light intensity of 50 μmol photons / (m^2 s) and growth has been monitored in the same way of the previous experiment. In Table 4.2 the pH value of the solutions before and after CO_2 bubbling are reported. The procedure regarding the CO_2 absorption protocol is detailed in the section §3.2.2, through the plot reported in Figure 3.10 the medium have been loaded and the CO_2 concentrations are known.

Table 4.2 *Represents the pH value of three different culture medium with three different sodium carbonate concentrations before and after the CO_2 bubbling.*

Na_2CO_3 (g/l) in the culture medium	Initial pH	Final pH
0	7.76	6.69
2.5	9.98	6.78
10	10.93	7.19

The plot reported in Figure 4.3(a) represents the variation of the fluorescence intensity over time.

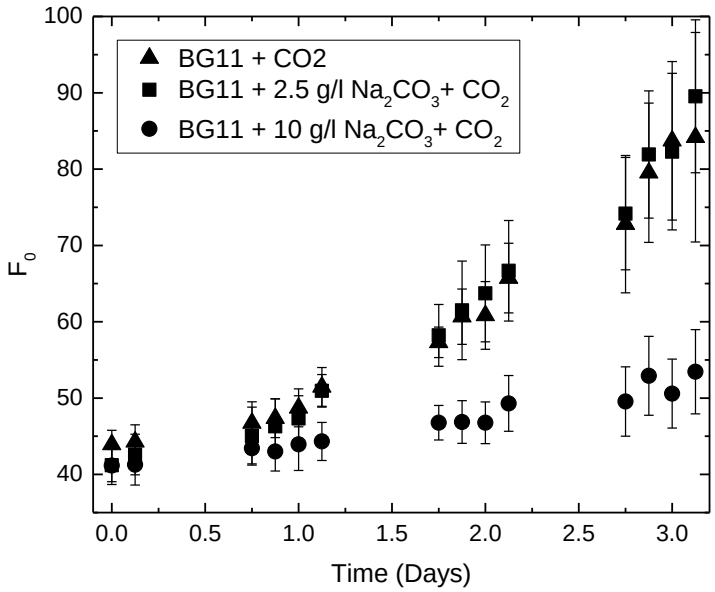

Figure 4.3*(a) Comparison of growth curves of Scenedesmus obliquus obtained using different concentration of sodium carbonate with CO_2 bubbling (0, 2.5, 10 g/l, represented respectively as triangles, squares, and circles). Plot showing the chlorophyll F_0 values as a function of time.*

The plot reported in Figure 4.3(a) represents the variation of the fluorescence intensity over time. *Scenedesmus obliquus* was able to utilize the CO_2 supplied in the medium by the bubbling system, which is also responsible for the lower pH data observed in Table 4.2.
Furthermore, it can be observed that a medium containing 2.5 g/l of Na_2CO_3 and loaded with CO_2 up to 6.78 pH, allowed the best microalgae growth in the exponential phase, it suggesting

that in these condition more CO_2 is absorbed and efficiently exploited by the biomass. The fluorescence intensity values have been elaborated in order to provide the growth curves in

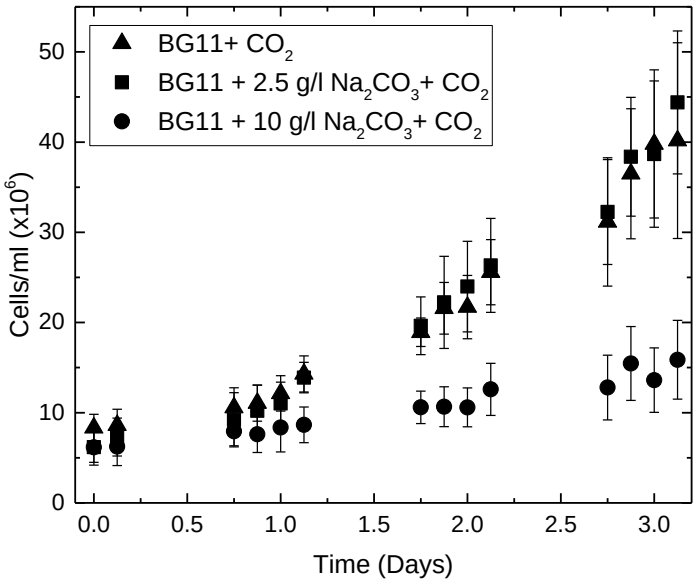

(b)

terms of cellular concentration (cell/ml ($\times 10^6$)) and the logarithmic fit of cellular concentration as a function of time (days).

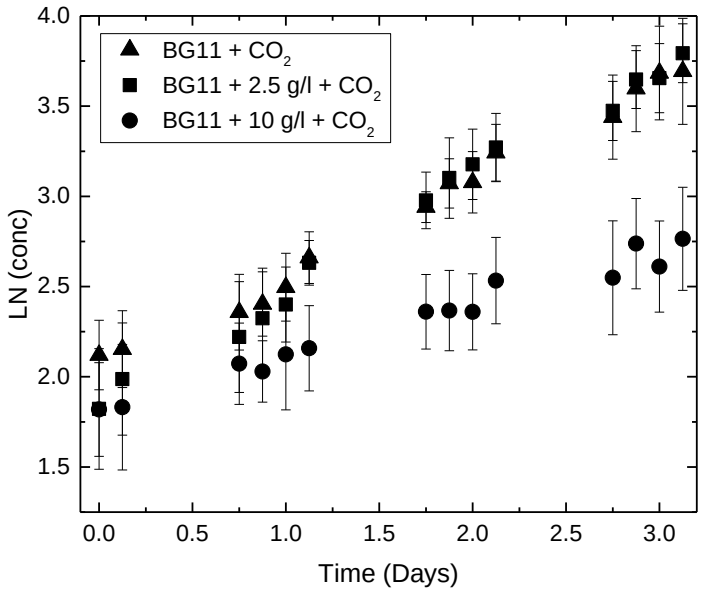

(c)

Figure 4.3 *Comparison of growth curves of Scenedesmus obliquus obtained using different concentration of sodium carbonate with CO_2 bubbling (0, 2.5, 10 g/l, represented respectively as triangles, squares, and circles).). (b) The plot showing the cellular concentration (cell/ml ($\times 10^6$)) as a function of time and (c) the plot showing the logarithmic fit of cellular concentration (cell/ml ($\times 10^6$)) as a function of time.*

The specific growth rates (Figure 4.3c) resulting are 0.32 d^{-1} for the BG11 with 10 g/l of Na_2CO_3, 0.56 for the BG11 and 0.68 for the BG11 with 2.5 g/l of Na_2CO_3. This suggest that increasing the concentration of CO_2 molecules in the medium, it can be directly exploited by microalgae as the carbon source (Gris *et al.*, 2014).

4.3 Experiment results BG11 2.5 g/l Na_2Co_3 with different light intensity

In order to evaluate the combined effect of several operating variables, microalgae growth with a culture medium with 2.5 g/l Na_2CO_3 and CO_2 at different light intensity was measured. The experiment was setup as for the previous tests, but the microalgae have been fed with the same culture medium (2.5 g/l Na_2CO_3 with CO_2 bubbling). It has been chosen to use the culture medium BG11 with 2.5 g/l of Na_2CO_3 and loaded with CO_2, because in the previously experiment had given the best response in terms of microalgal growth. To this aim specific photo-filters (ND) were overlaid to the micro-PBR in order to decrease the light intensity for specific micro-PBR sections. The photo-filers were properly chosen to cut between 30 and 50% of the light intensity. This allow controlling the irradiance reaching different wells on the same device simultaneously. This design allowed obtaining three sections of the chip with 40 (low light), 75 (medium light) and 145 (high light) μmol photons/(m^2 s) intensities, respectively, by using a single fluorescent white light source with eight biological replicates for each condition. Growth was monitored over time according to the method described in section §2.4.

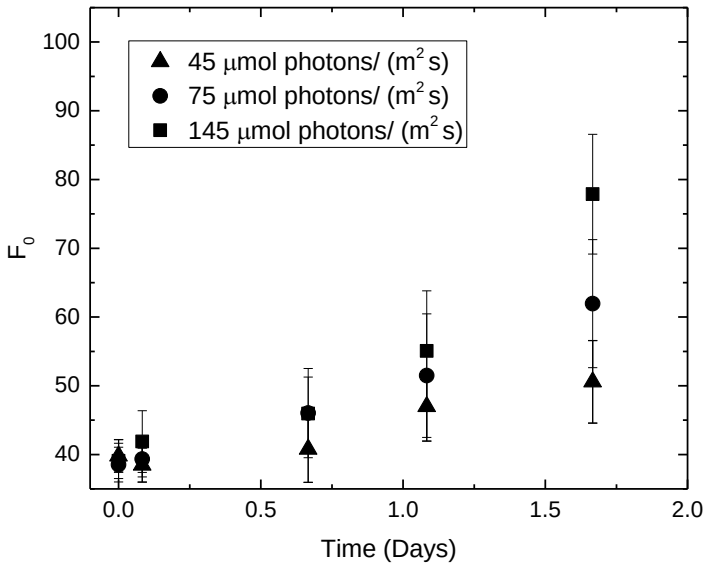

Figure 4.4*(a) Comparison of growth curves of Scenedesmus obliquus obtained using different light intensity at the same culture medium 2.5 g/l Na_2CO_3 with CO_2 (45, 75, 145 μmol photons/(m^2 s), represented respectively as triangles, circles, and squares). Plot showing the chlorophyll F_0 values as a function of time.*

The data (Figure 4.4) showed that light intensity has a huge impact on growth. By enhancing the light intensity, cultures grew proportionally faster. Since they show increasing growth according to the light intensity increase, this confirms that cultures in the micro-PBR are not limited by the CO_2.

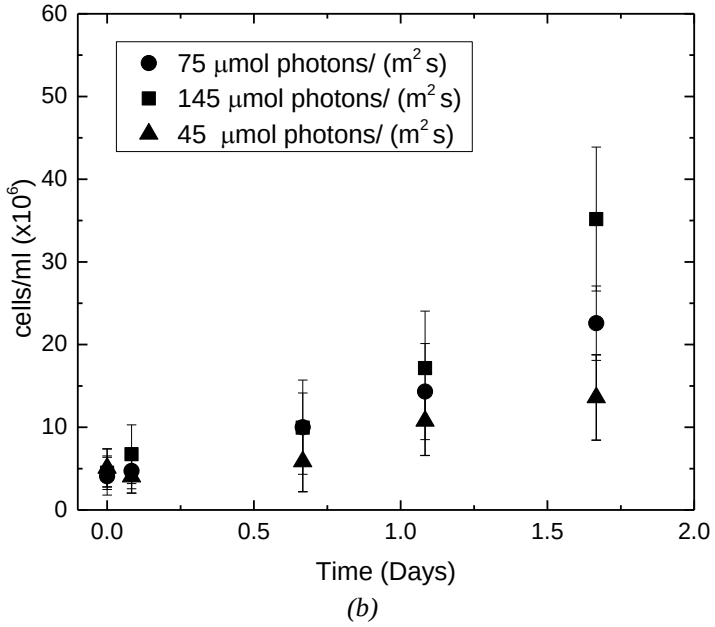

(b)

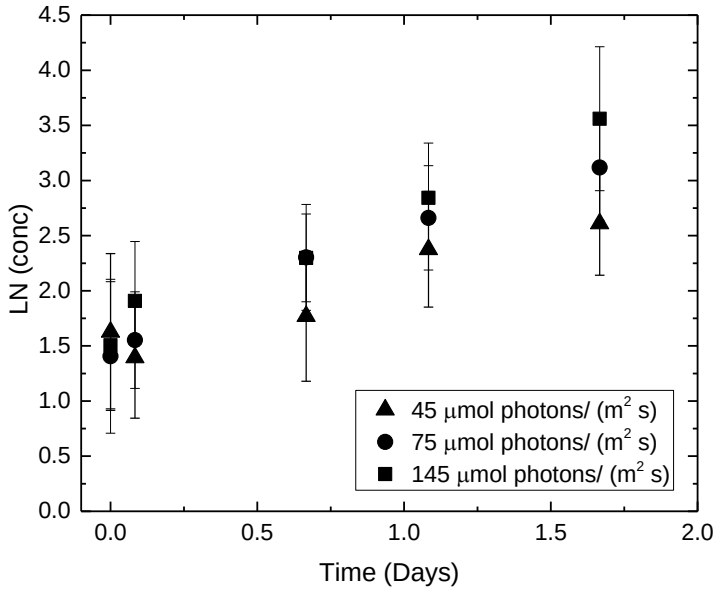

(c)

Figure 4.4 *Comparison of growth curves of Scenedesmus obliquus obtained using different light intensity at the same culture medium 2.5 g/l Na_2CO_3 with CO_2 (45, 75, 145 μmol photons/(m^2 s), represented respectively as triangles, circles, and squares). (b) The plot showing the cellular concentration (cell/ml (× 10^6)) as a function of time and (c) the plot showing the logarithmic fit of cellular concentration (cell/ml (× 10^6)) as a function of time.*

The plots in Figure 4.4 indicate that, microalgae cells exposed to high light condition (145 μmol photons/(m^2 s)) showed a slight but a significant increase in the specific growth rate (Figure 4.4c). This was expected, considering that the influence of light on microalgae growth is extremely important and also the values obtained is similar than data reported in literature (Perin *et al.*, 2016).

Conclusions

This Thesis was aimed at designing an efficient CO_2 supply system for microalgae growth in a microphotobioreactors.

The first part of this work was characterized by some preliminary analysis of the microPBR configuration. The purpose was to firstly assess the contribution of carbon dioxide, through the nutrient flow, to the microalgae with a qualitative and quantitative approach. Taking as reference the micro-PBR used in the previous work by Baseotto (Figure 3.1), preliminary study on CO_2 limitation was carried out. Two balances were applied, one concerning the microchannel that connects the well to the feed channel and one based on the well. Based on the known concentration of carbon dioxide inside the channel, CO_2 normally dissolved in a liquid under standard condition (ambient temperature and pressure) was calculated. A CO_2 concentration equal to 4.4×10^{-4} g/l, which is that one in equilibrium with air, resulted far lower than that required in the channel (0.3 g/l) to operate in non-limiting CO_2 conditions.

It was therefore necessary to evaluate a method for absorbing a sufficient amount CO_2 inside the BG11 culture medium.

In order to quantitatively establish the gas CO_2 concentration needed to obtain such a concentration in the culture medium, a sensitivity analysis was carried out. To quantify with reliable methods the CO_2 amount in the liquid, a software able to study the liquid-gas equilibria was used. The liquid concentration and equilibria have been studied by varying the ratio air/CO_2 in the inlet flow. A 100% CO_2 flow was chosen as the best value.

With the increase of the CO_2 dissolved in water, the carbonic acid increases with a consequent decrease in the pH that may affect algae growth. To overcome this problem, the solution was buffered with carbonate and bicarbonate, compatibles with microalgae growth. First, the effect of both sodium bicarbonate and carbonate has been evaluated, changing the concentration up to 0.4M and keeping the CO_2 flow constant. Taking into account the use in future experimentation of microalgae that require a saline medium, the tests have been carried out also for seawater this has been simulated by adding 30 g/L of NaCl.

Sodium carbonate has been then for experiments used, as it allows a greater absorption of C in the liquid (17 g/l), with pH values (pH = 7) compatible with the microalgae optimal growth conditions. By adding carbonates to the BG11 medium the equilibria is shifted and the overall results is an increase amount of carbon in the medium.

Finally, a new micro-PBR that allowed to investigate the efficiency of a medium with higher CO_2 concentrations on microalgae growth has been designed and characterized.

In order to assess the influence of carbon dioxide on the microalgae growth objectively, two experiments have been performed, with and without addition of CO2 in the culture medium (BG11).

The microalgae growth has been measured through *in vivo* chlorophyll fluorescence measurements, and a preliminary correlation between cell concentration and fluorescence intensity has been found.

Experiments demonstrated that *Secenedesmus obliquus* is not able to use carbonate ions itself with high efficiency, probably due to the increase pH of the medium, which inhibits the growth. However, a significant growth was achieved by loading CO_2 in the culture medium buffered with sodium carbonate; this allowed controlling the pH of the culture system, and thus shifting the carbonate equilibria in favour of free CO_2 efficiently exploited by *Scenedesmus obliquus*.

In summary, in this growth system *Scenedesmus obliquus* is not limited by the CO_2 availability, therefore confirming the full compatibility of the micro-PBR with the microalgae growth.

In accordance with the results, microalgae growth with a culture medium with 2.5 g/l Na_2CO_3 and CO_2 at different light intensity was measured. Light availability has a huge impact on photosynthetic growth, and therefore the monitoring of the photosynthetic performances when cells are exposed to different light regimes is a valuable source of information to optimize their culture system. The results indicate that, microalgae cells exposed to high light condition (145 μmol photons/(m^2 s)) showed a significant increase in the specific growth rate.

The simultaneous growth monitoring in three different light regimes and with three different culture medium was used to demonstrate the method applicability for high-throughput studies. In fact, where compared to traditional methodologies, the data generation capability of such a micro-PBR is extremely increased. Algae showed fast growth rates, this allowing less time-consuming experiments, in addition, the micro-PBR has the capability of simultaneously testing multiple variables (light intensity and salt concentration). Reproducing the same experiments, using traditional techniques would dramatically lengthen the timespan. Another advantage is that nutrients and chemicals consumption is strongly reduced.

The possible future implications concern the possibility to study the microalgae growth of a saline species (*Nannochloropsis gaditana*) in non-limiting CO_2 conditions. Furthermore, the correlation (F_0 – cells concentration) used in this work has been obtained through three different calibrations carried out with microalgae acclimatized to different conditions, for this reason this is a preliminary correlation and will have to be investigated in the future.

Finally, given the advantages of the designed micro-PBR, in the near future it will be possible optimize the design, redesigning the closing unit in order to guarantee a homogeneous flow and avoid possible losses of medium.

Bibliography

Allakhverdiev, S. I., A. Sakamoto, Y. Nishiyama, M. Inaba and N. Murata (2000). *«Ionic and Osmotic Effects of NaCl-Induced Inactivation of Photosystem I and II in Synechoccus»*. American society and Plant Biologists, **123**, 1047-1056.

Baseotto N. (2016). *«Sviluppo di un sistema a flusso continuo per la crescita di microalghe in una matrice di microfotobioreattori»*. Tesi di Laurea Magistrale in Ingegneria Chimica e dei Processi Industriali. Università degli Studi di Padova.

Becker, E. W. (1994). *«Microalgae: Biotechnology and Microbiology»*, (1st ed.), Cambridge University Press.

Boelee, N.C., H. Temmink, M. Janssen, C.J.N. Buisman, R.H. Wijffels. (2014) *«Balancing the organic load and light supply in symbiotic microalgal-bacterial biofilm reactors treating synthetic municipal wastewater»*, Ecological Engineering, **64**, 213–221.

Bona F., A. Capuzzo, M. Franchino, M. E. Maffei (2014). *«Semicontinuous nitrogen limitation as convenient operation strategy to maximize fatty acid production in Neochloris oleoabundas»*, Algal Research, **5**, 1-6.

Borowitzka, M. A. (2005). *«Culturing microalgae in outdoor ponds»*. In: Algal Culturing techniques, Elsevier Academic Press, 202-218.

Cai, Y., W. Wang, L. Li, Z. Wang, S. Wang, H. Ding, Z. Zhang, L. Sun, W. Wang (2018). *«Effective Capture of Carbon Dioxide Using Hydrated Sodium Carbonate Powders»*. MDPI, Materials, **11**, 183.

Castaldello, C., (2018). *«Report 1»*, PhD student, University of Padova.

Cheong, SH., MY. Kim (2010). *«Spirulina prevents atherosclerosis by reducing hypercholesterolemia in rabbits fed a high-cholesterol diet»*. In: J Nutr Sci Vitaminol, Tokyo, **56(1)**, 34-40.

Chisti, Y. (2007). *«Biodiesel from microalgae»*, Biotechnology advances, **25**, 294-306.

Concas, A., G. A. Lutzu, M. Pisu, G. Cao (2012). *«Experimental analysis and novel modeling of semi-batch photobioreactors operated with Clorella vulgaris and fed with 100% (v/v) CO_2»*, Elsevier, **213**, 203-213.

Cussler, E. L. (1997). *«Diffusion: Mass transfer in Fluid System»*. (2nd ed.), Cambridge University Press.

Di Martino, V. and B. Stancanelli (2015). *«Colture indoor di microalghe finalizzate alla produzione di biomasse da destinare a produzioni zootecniche e bio-energetiche»*, ISAFoM-CNR UOS di Catania, 2-10.

Ding, G.T., Z. Yaakob, M.S. Takriff, J. Salihon, M. S. Abd Rahaman (2015). *«Feasibility of the optical density (OD) in the determination of the microalgal biomass using palm oil mill effluent (POME) as medium»,* International Journal of Hydrogen Energy, **41**, 4888-4895.

ELVESYS R&D team:

- (2018a). *Microfluidics: a general overview of microfluidics.* URL: https://www.elveflow.com/microfluidic-tutorials/microfluidic-reviews-and-tutorials/microfluidics/ (last accessed 23/04/2018).
- (2018b). *Microfluidics: a general overview of microfluidic: A review.* URL: http://www.elveflow.com/microfluidic-tutorials/microfluidic-reviews-and-tutorials/microfluidics-and-microfluidic-device-a-review/ (last accessed 23/04/2018).
- (2018c). *PDMA: A review.* URL: https://www.elveflow.com/microfluidic-tutorials/microfluidic-reviews-and-tutorials/the-poly-di-methyl-siloxane-pdms-and-microfluidics/ (last accessed 23/04/2018).
- (2018d). *Pulsation and oscillation of syringe pumps in microfluidics.* URL: http://www.elveflow.com/microfluidic-tutorials/microfluidic-reviews-and-tutorials/syringe-pumps-and-microfluidics/stability-and-flow-oscillation-of-syringe-pumps-in-microfluidic/ (last accessed 28/04/2018)
- (2018e). *Pulsation and oscillation of syringe pumps in microfluidics: A review.* URL: http://www.elveflow.com/microfluidic-tutorials/microfluidic-reviews-and-tutorials/microfluidics-and-microfluidic-device-a-review/ (last accessed 28/04/2018).

Encyclopaedia Britannica:

- (2018a). *Diatom.* URL: https://www.britannica.com/science/diatom (last accessed 15/05/2018).
- (2018b). *Green algae.* URL: https://www.britannica.com/science/green-algae (last accessed 15/05/2018).
- (2018c). *Golden algae.* URL: https://www.britannica.com/science/golden-algae (last accessed 15/05/2018).
- (2018d). *Yellow-green algae.* URL: https://www.britannica.com/science/yellow-green-algae (last accessed 15/05/2018).

Foley, P. M., E. S. Beach, J. B. Zimmerman (2011). *«Algae as a source of renewable chemicals: opportunities and challenges»*. Green Chemictry, **13(6)**, 1399-1405.

Gris, B., E. Sforza, L. Vecchiato and A. Bertucco (2014). *«Development of a Process for an Efficient Exploitation of CO_2 from Flue gases as Liquid Carbonates for Chlorella protothecoides Cultivation»*. I&EC research, American Chemical Society, **53**, 16678-16688.

Guendales, A. C., H. M. Amaro, F.X. Malcata (2010). *«Microalgae as source of high added-value compounds»*. In: Biotechnology Progress, **3**, 597-613.

Harvard Apparatus: syringe pump PHD ULTRA™ (2018). URL: https://www.harvardapparatus.com/pumps-liquid-handling/syringe-pumps/infuse-withdraw/standard-infuse-withdraw-phd-ultra-syringe-pumps.html (last accessed 2/05/2018).

Ho, S., C. Chen, D. Lee, J. Chang (2011). *«Prospectives on microalgae CO_2-emission mitigation systems-A review»*. In: Biotechnology Advances, **29**, 189-198.

Lavens, P., P. Sorgeloos (1996). *«Manual on the production and use of live food for aquaculture»*. FAO, Fisheries Technical Paper.

Lee, Y. K. (2016). *«Microalgae Cultivation Fundamentals»*. In: Algae Biotechnology - Products and Processes. A cura di Faizal Bux e Yusuf Chisti, 1– 18.

Leite, G.B., A. E. Abdelaziz, P. C. Hallenbeck (2013). *«Algal biofuels: Challenges and opportunities». In:* Bioresour Technol, **145**, 134-141.

Lower, S. K. (1999). *«Carbonate equilibria in natural waters*», Chem1 Enviromental Chemistry, Simon Fraser University.

Masojídek, J., M. Koblížek, G. Torzillo (2004). *«Photosynthesis in Microalgae»*. In: Handbook of Microalgal Culture: Biotechnology and Applied Phycology. A cura di Amos Richmond. Blackwell Science, 20–37.

Mata, T. M., A. A. Martins, N.S. Caetano (2010). *«Microalgae for biodiesel production and other applications: A review»*. In: Renewable and sustainable Energy Reviews, **14**, 217-232.

McCormick, M. J., G. L. Fahnenstiel, S. E. Lohrenz, D. G. Redalje (1996). *«Calculation of cell-specific growth rates: A clarification»*. In: Limnology & Oceanography, ASLO Wiley, **41**, *182-189.*

McDonald, J. C., D.C. Duffy, J.R. Anderson, D.T. Chiu, H. Wu,O. J. A. Schueller, G. m: Whitesides (2000). *«Fabrication of microfluidic system in poly(dimethylsiloxane)»*. Electrophoresis 2000, **21**, 27-40.

Medipally, S. R., F. M. Yusoff, S. Banerjee, M. Shariff (2015). *«Microalgae as Sustainable Renewable Energy Feedstock for Biofuel Production»*. In: BioMed research International, Hindawi publishing Corporation, 1-9.

Monetti, F. (2016). *«Sviluppo di microfotobioreattori per la crescita di microalghe»*. Tesi di Laurea Magistrale in Ingegneria Chimica e dei Processi Industriali. Università degli Studi di Padova.

Murchie, EH. And T. Lawson (2013). *«Chlorophyll fluorescence analysis: a guide to good practice and understanding some new applications»*. In: Journal of Experimental Botany, **64**, 3983-3998.

Nelson, D. L. and M. M. Cox (2006). *«Lehninger principles of biochemistry»*, (4^{th} ed.), W. H. Freeman and Company, New York.

Nguyen, N.-T. and S. T. Wereley (2006). *«Fundamentals and Applications of Microfluidics»*, (2nd ed.), Artech house, Boston (U.S.A), 1-8.

Noel Vinaly, T., Se-Kwon K. (2013). *«Beneficial Effects of Marine Algal Compounds in Cosmeceuticals»,* US National Library of Medicine National Institute of Health, **11**, 146-164.

OPEC (2015). URL: http://www.opec.org/opec_web/en/ (last accessed 20/05/2018).

Patel, A., B. Gami, P. Patel, B. Patel (2017). *«Microalgae: Antiquity to era of integrated technology»,* Renewable and sustainable energy sources, **71**, 535-547.

Perin, G., E. Cimetta, F. Monetti, T. Morosinotto, F. Bezzo (2016). *«Novel micro-photobioreactor design and monitoring method for assessing microalgae response to light intensity»,* Algal Researches, Elsevier, **19**, 69-76.

Proto Labs (2018). *Stereolithography* URL: https://www.protolabs.co.uk/services/3d-printing/stereolithography/ (last accessed 24/04/2018).

Qin, D., Y. Xia, G. M. Whitesides (2010). *«Soft lithography for micro- and nanoscale pattering»,* Nature Publishing Group, **3**,491-502.

Richmond, A. (2004). *«Handbook of Microalgae Culture: Biotechnology and Applied Phycology»*. (1st ed.), Blackwell Publishing Ltd, Australia.

Sano Coelho, R. (2017). *«Biodiesel production from heterotrophic microalgae»,* Universidade Estaual de Campinas, Brazil, 5-7.

Sayin, I., C. Cingi, F. Oghan, B. Baykal, S. Ulusoy (2013). *«Complementary therapies in allergic rhinitis»,* ISRN Allergy, **13**.

Sforza, E., (2012). *«Oil from microalgae: species selection, photobioreactor design and process optimization»*. In Ph.D. Thesis – Padua University.

Shim, J. G., D. W. Lee, J. H. Lee, N. S. Kwak (2016). *«Experimental study on capture of carbon dioxide and production of sodium bicarbonate from sodium hydroxide»*. Korean Society of Environmental Engineers, **21(3)**, 297-303.

Staehelin, L. A. and C. J. Arntzen (1986), «*Encyclopedia of Plant Physiology»*, **19**, 1-84.

Taiz, L. and E. Zeiger (2010). *«PLANT PHYSIOLOGY»*. (5rd ed.), Sinauer Associates Inc.

UCMP:

- (2018a). *Introduction to the Rhodophyta – the red "algae".* URL: http://www.ucmp.berkeley.edu/protista/rhodophyta.html (last accessed 15/05/2018).
- (2018b). *Introduction to the Phaeophyta – kelps and brown "algae".* URL: http://www.ucmp.berkeley.edu/chromista/phaeophyta.html (last accessed 15/05/2018).
- (2018c). *Introduction to the Cyanobacteria – Architects of earth's atmosphere.* URL: http://www.ucmp.berkeley.edu/bacteria/cyanointro.html (last accessed 15/05/2018).

Whitesides, G. M. (2006). *«The origins and the future of microfluidics»*, Nature, International journal of science, **442**, 368-373.

List of Figures

List of Tables